Helium separation using membrane technology: Recent advances and perspectives

Zhongde Dai[1*], Jing Deng[2*], Xuezhong He[3*], Colin A. Scholes[4], Xia Jiang[1], Bangda Wang[1],

Hongfang Guo[1], Yulie Ma[1], Liyuan Deng[5*]

1. College of Architecture and Environment, National Engineering Research Centre for Flue
    Gas Desulfurization, Sichuan University, 24 south Section 1 Ring Road No.1 Chengdu
    610065, China
2. School of Chemical, Biological and Materials Engineering, University of Oklahoma,
    Norman, 73019, USA
3. Department of Chemical Engineering, Guangdong Technion-Israel Institute of Technology
    (GTIIT), 241 Daxue Road, Shantou, 515063, China
4. Department of Chemical Engineering, University of Melbourne, Victoria 3010 Australia
5. Department of Chemical Engineering, Norwegian University of Science and Technology,
    NO-7491, Norway
Corresponding authors:
Zhongde Dai, zhongde.dai@scu.edu.cn
Jing Deng, Jing.Deng-1@ou.edu
Xuezhong He, xuezhong.he@gtiit.edu.cn
Liyuan Deng, deng@nt.ntnu.no

Abstract:

Helium is an unrenewable noble gas produced from natural gas with a wide range of scientific, medical, and industrial applications. Due to the large differences in the kinetic diameters between helium (0.26 nm) and nitrogen (0.364 nm) or methane (0.38 nm), membrane technology has been considered a promising alternative to traditional technologies for helium recovery and purification. This paper systematically reviews the advances in membrane material development for helium separation in recent years. Gas permeation data presented in this work were collected from over 1000 membrane materials, including polymeric, inorganic, and mixed matrix membranes. Moreover, membrane processes for helium recovery and purification from natural gas were

critically analyzed and discussed concerning technical feasibility, energy consumption, and separation costs. Challenges in helium purification using membrane technology were also discussed, and potential solutions have been suggested. Lastly, future perspectives on research directions on membrane material development and hybrid helium purification process design and optimization are proposed.

Keywords:

Helium recovery; membrane separation; polymeric membranes; carbon molecular sieve membranes; inorganic membranes; hybrid processes

Graphic abstract：
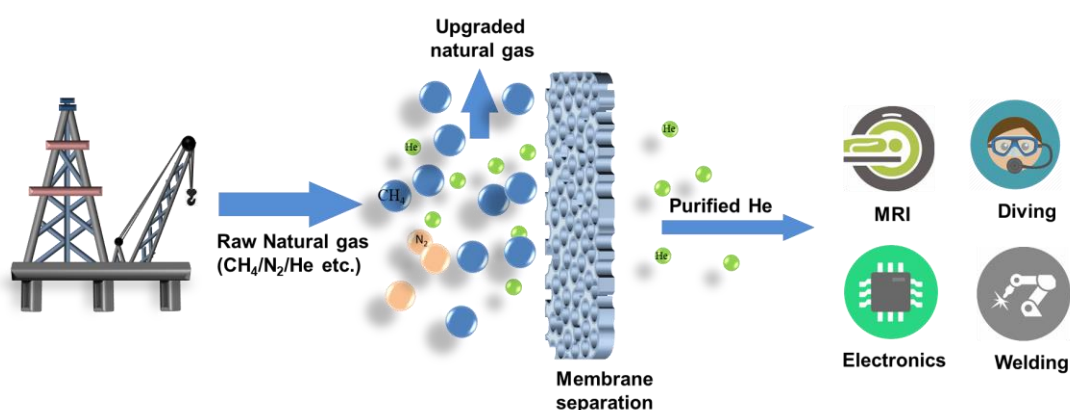
Highlights

- An overview of recent advances in helium separation membranes and processes is presented.
- Helium separation performances of more than 1000 membrane materials are summarized and analyzed.

- Strengths and challenges of membrane processes for helium recovery and purification from natural gas are critically analyzed.

- Future research directions in membrane materials and processes for helium separation are proposed.
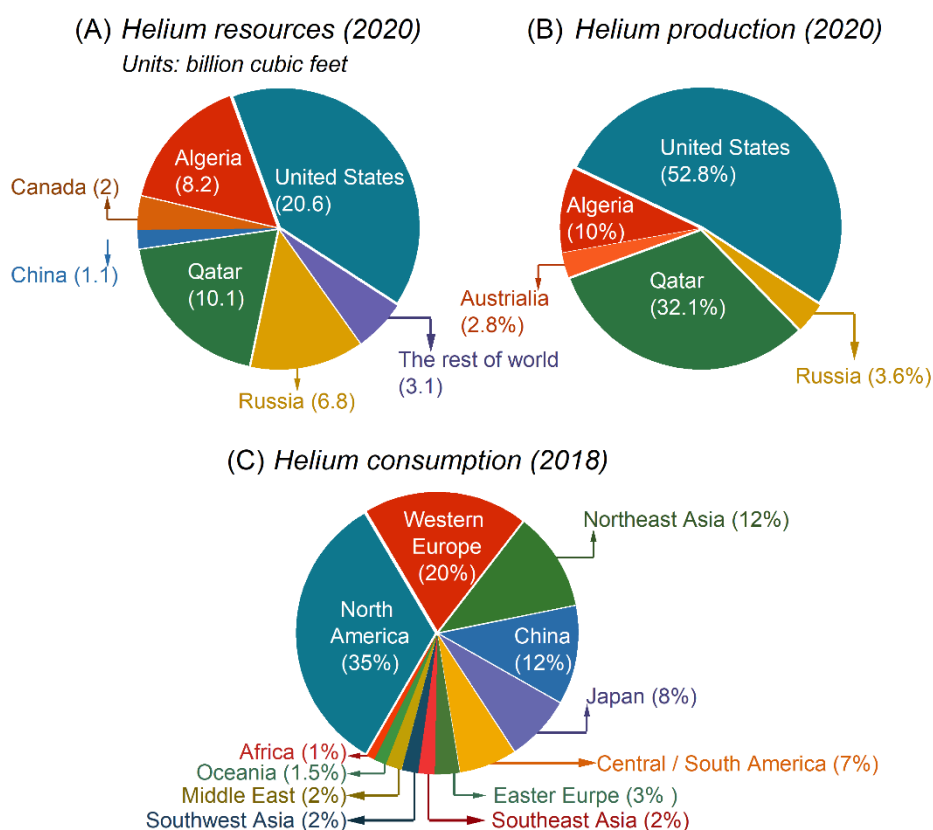
Outlines

1. Introduction

Helium is a colorless, odorless, tasteless, non-toxic, chemically inert, and nonflammable gas that heads the noble gas group in the periodic table. Helium has the lowest boiling point among all known materials, gets liquefied at -269 °C, and remains liquid at about absolute zero [1]. It is also the second lightest gas, slightly heavier than H_2. Due to these intrinsic properties, helium has gained widespread applications in the medical, nuclear, and space industries. More specifically, in some of these applications (e.g., nuclear magnetic resonance imaging, NMRI [2]), there is no other substitute for helium [3, 4]. Thanks to its inert nature, high specific heat, and thermal conductivity, helium is also widely used as welding protective gases, coolants in fiber optic cable manufacturing, and working gas in lasers and lighting [5]. Laboratories usage, such as carrier gas for gas chromatography, powder carrier gas for thermal spraying, cold spraying, and use in thermoacoustic heat pumps are other fields of helium applications [1]. Important applications for helium also include pressurizing liquid fuel for missiles [6, 7], deep-sea divers breathing mixtures to avoid nitrogen narcosis [8-10], lighter-than-air systems [3, 11-13], and leak detection [14, 15]. The most well-known party application (i.e., filling balloons) has only contributed to about 8 % of helium's total consumption worldwide. The distribution of helium consumption by applications is shown in **Figure 1** [16].
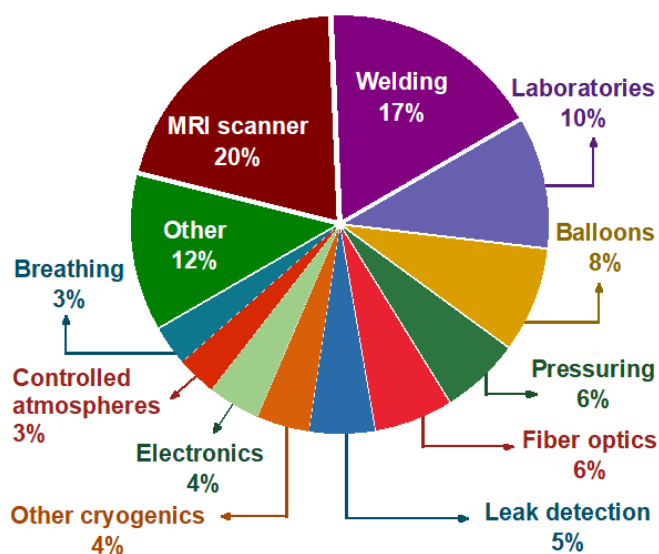
Figure 1. Distribution of helium consumption worldwide by applications [16, 17].

1.1 He sources, supply and consumption

Helium is the second most abundant element in the observable universe, but it is not rich on earth. Up to now, the only commercially viable helium source is helium-containing natural gas [18]. The global distribution of helium reservoirs is shown in **Figure 2A**. Most helium-rich reservoirs are located in only a handful of countries, such as the USA, Qatar, and Russia. Recently, new reservoirs have been found in Africa (e.g., Tanzania) and North America (e.g., Canada). But so far, the USA, Qatar, Algeria, and Russia still hold about 90 % of the total helium reservoirs. Interestingly, the definition of helium-rich NGs varies in different countries. In the United States, natural gas with a helium concentration of higher than 0.3 % is considered helium-rich and commercially profitable to be recovered [16], while in Russian, this value is 0.05 % [11].

(A) *Helium resources (2020)*
Units: billion cubic feet

(B) *Helium production (2020)*

(C) *Helium consumption (2018)*

Figure 2. The distribution of global helium reserves (A) and helium production (B) in 2020, data was obtained from Ref. [19]. Helium consumption's distribution is presented in (C) with data from Ref. [20].

In 2020, more than 50 % of the helium is produced in the USA [19, 21] (**Figure 2B**) and 32 % in Qatar. The rest of the helium production is mostly in Algeria and Australia. Therefore, most of the helium consumption countries need to import helium from either the USA or Qatar.

To date, about 30,000 tons of helium is consumed annually, which translates to a US$ 1 billion worth of global market. **Figure 2C** [20] clearly shows that North America is the largest helium consumer in the world and Western Europe comes as the 2nd, with their total market shares accounting for more than half of the total helium consumption globally, most likely due to their large medical and manufacturing needs. Noticeably, as a small country, Japan consumes approximately 8% of helium globally, possibly resulted by its advanced electronic industries. Some countries, such as China and Japan, also consume a significant amount of helium but with almost zero production

6

contribution.

Future projection estimates an increase in helium demands of about 6 % per year, especially in the semiconductor and medical sectors [11]. As such, the helium shortage has been considered a critical issue not only for scientific research but also in industries and daily life in the near future [22-25]. In February 2018, when two of the world's major supply countries, the USA and Qatar, began to allocate supplies to their contract customers, there came the so-called "Helium Shortage 3.0" [26, 27]. Even though the situation has been slightly eased due to the pandemic in 2020, the shortage is continuing.

1.2 He recovery technologies

As mentioned above, helium-rich natural gas is the only source for helium production currently. Typical gas components in natural gas include methane (70~90 %), C_2-C_3 hydrocarbons (0~20 %), heavy hydrocarbons (1~3 %), CO_2 (0~10 %), nitrogen (0~10 %), and a small amount of hydrogen sulfide and helium [18]. In a typical natural gas process, impurities, such as H_2S, CO_2, H_2O, and heavy hydrocarbons, in crude natural gas need to be removed to prevent them from corroding pipelines and equipment and also to meet calorific value regulations for natural gases.

The remaining gas, containing N_2, CH_4 and a small amount of inert gas, is sent to an N_2 rejection unit to collect CH_4, which is Option A in **Figure 3**. After most CH_4 is removed, nitrogen becomes the major component in the gas stream. A helium recovery unit is then applied to concentrate helium from 1~3% to 50~70% (also named as 'crude' helium) [19], and the helium-rich product is sent to a helium upgrading unit for further purification. Another plan (Option B) has been proposed recently to provide the possibility to retrofit the existing natural gas plant without interfering with the remaining gas upgrading process easier incorporated into current facilities [28], which is to extract helium directly from natural gas after the pre-treatments of dehydration and sweetening processes (see **Figure 3**). However, noteworthy, the gas volume needed to be dealt with in the helium recovery unit will be largely higher than the current ones. Due to this, it is still not applied in real-life conditions.

It is worth mentioning that the helium recovery and upgrading units are unnecessary to be located in the same place. For instance, fourteen plants form different states, USA, extract helium from natural gas and produce crude helium ranging from 50 to 90 %. The crude helium is then sent to three plants in Kansas and one in Oklahoma for further purification to produce Grade-A helium (99.997 % or higher) [19].
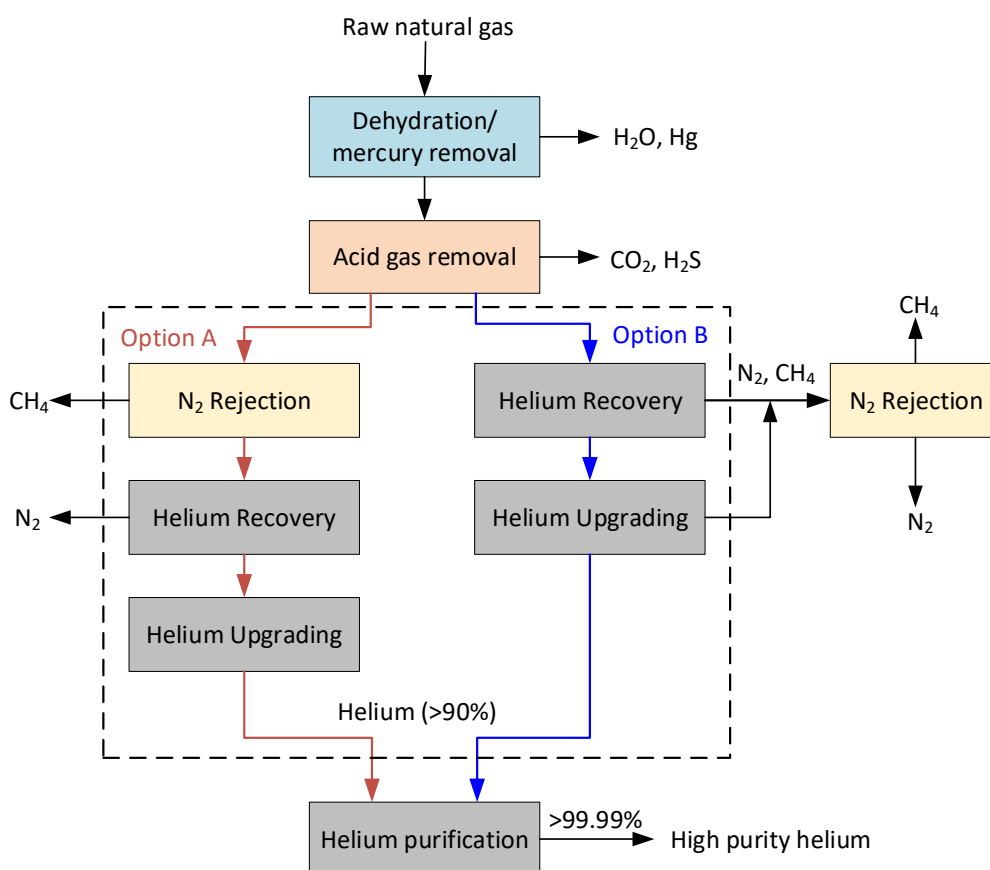
Figure 3. Process illustration of helium production from natural gas (replotted based on ref [18, 28] with permission). Copyright (2017) from Elsevier.

Different technologies, such as cryogenic distillation, pressure swing adsorption (PSA), membrane gas separation, and hybrid systems, can be employed for helium recovery from natural gas [18, 29]. The choice of a suitable process largely depends on the gas volume flow and the feed composition. Currently, cryogenic separation is the only method used for large-scale helium recovery, followed by PSA for further upgrading (> 90% helium) [18]. However, since helium is the least condensable compound in the stream (boiling point: -268.9 °C), the other gas species (i.e., N_2 and/or

CH$_4$) , which account more than 90 mol% of the feed stream, need to be liquefied to achieve efficient separation. Therefore, significantly large energy needs to be consumed to obtain only crude helium. In addition to the operational cost, the capital cost of these cryogenic distillation columns is also considerable. Both of these factors hinder the growth of the helium recovery plant and also its production. Besides, as nations pursue clean energy, it is expected that the production of natural gas will decrease in the coming future, which will inevitably affect helium production. This will cause a greater gap between helium production and its demand, which is increasing at a rate of ~ 6%/year.

The lower cost of the helium recovery unit, on both capital and operation sides, is greatly beneficial for addressing this issue. Another path is lowering the current limitation of helium concentration in natural gas field by advanced extraction technologies, which can turn more natural gas fields into available sources for helium production. But this requires the separation method to be more efficient in extract helium from the lean stream. Therefore, developing new technologies that can more efficiently extract and purify helium is highly desired.

Owing to the large differences in kinetic diameter between helium (2.6 Å) and other components of natural gas (e.g., 3.8 Å for CH$_4$ and 3.64 Å for N$_2$), membrane technology became a feasible alternative to conventional technologies for helium separation from natural gas as early as the 1960s [30]. Helium permeates while the rest of the feed gas permeates slower than helium through the membrane. This process does not rely on phase changes and hence consumes much less energy, compared to cryogenic distillation. Membrane separation also possesses several engineering advantages, such as small footprint, simple operation, no moving parts, and low environmental impacts [31]. Around 1980, the first commercial helium extraction unit based on membrane technology was installed, which consumed only about 40 % energy of the cryogenic process [32]. Since then, extensive research has been carried out on membrane-based helium separation [33]. Different membrane materials such as polymeric materials, inorganic materials, carbon membranes, and mixed matrix membranes (MMMs), have been developed for this application [34]. In 2016 and 2017,

several studies reviewed the progress on membrane technology for helium recovery/separation [35-37].

Nevertheless, breaking-throughs in novel materials, especially the emerging novel polymer and inorganic nano-structure materials, have made a blowout growth in new membrane materials for helium separation in recent years. Moreover, a tremendous number of membrane-based helium purification processes, including membrane processes and hybrid processes combining the membrane and other technologies, have been reported for significant improvement through process optimization by modeling and simulation. Therefore, a critical review of helium separation with a summary of the recent progress in this field is highly needed.

This review provides a brief introduction to the helium application and production, focusing on the recent progress in novel helium-separation membrane materials. Advances in polymeric membranes for helium separation were firstly summarized and analyzed, followed by carbon membranes, inorganic membranes, and mixed matrix membranes. The technology advances and economic feasibility of membrane technology with other stand-alone or hybrid processes for helium recovery were also analyzed and compared. Finally, future perspectives on membranes for helium recovery concerning novel material development and upscaling, process design, and optimization are proposed.

2. Membrane materials for helium separation

2.1 Basic principles

Gas separation membranes rely primarily upon two parameters, i.e., permeability and selectivity. Gas permeability is the normalized gas flux through a membrane multiplied by the membrane thickness, which indicates how fast a gas penetrates through a membrane, generally with a unit of Barrer (1 Barrer= 10^{-10} cm^3 (STP) cm cm^{-2} s^{-1} cmHg^{-1}). Other SI units have also been widely used (e.g., mol m m^{-2} s^{-1} Pa^{-1}), especially for

inorganic membranes. Gas permeability can be calculated via equation (1):

$$P_i = \frac{N_i l}{\Delta p} \qquad (1)$$

where P_i is the gas permeability, N_i is the steady-state flux through the membrane, l

is the membrane thickness, and Δp is the partial pressure difference of gas i between

the feed side and permeate side.

Selectivity is the indication of the ability of the membrane to separate different gas

species. One of the commonly used selectivity is called "ideal selectivity", which is

defined as the ratio of two gases' permeabilities in equation (2).

$$\alpha_{ij}^* = \frac{P_i}{P_j} \qquad (2)$$

where α_{ij}^* is the ideal selectivity of gas i over j .

In mixed gas permeation tests, instead of the ideal selectivity, separation factor, as

defined in equation (3), is widely used.

$$\alpha_{i/j} = \frac{y_i / y_j}{x_i / x_j} \qquad (3)$$

where $\alpha_{i/j}$ is the separation factor of gas i over j , y_i and y_j are the mole fractions of

gas i and j in the permeate stream, while x_i and x_j are the mole fractions of gases i

and j in the feed side, respectively.

For polymeric membranes, helium separation is dominatingly based on the solution-

diffusion mechanism. Gas mixtures can be separated by membrane due to their

differences in solubility and diffusivity in the polymeric membrane matrix. On the other

hand, for porous inorganic membranes, the helium separation mechanism is based

solely on molecular sieving. Due to the inert nature of helium, surface diffusion or

capillary condensation are not likely to occur; thus, by precisely controlling pore size,

the selectivity of helium over other gases can be much higher in inorganic membranes

compared with that in polymeric membranes.

2.2 Gas Transport mechanisms in membranes

Generally, there are three models to describe the gas transport in membranes. The first one is the pore-flow model, in which gas molecules are transported by pressure-driven convective flow through pores in the membrane. Separation can be obtained because some of the permeants is excluded (filtered) from some of the pores while others could pass; The second model is called solution-diffusion model, in which gas molecules firstly dissolve in the membrane material and then diffuse through the membrane, separation occurs between different gases due to their differences in either solubility or diffusivity. The third one is called facilitated transport model. In this process, normally a reversible reaction happens between the membrane material and the gases. Separation can be achieved due to the reaction kinetic differences. To the best of the authors knowledge, there is no facilitated transport reported for He separation, thus only pore-flow model and solution-diffusion model was described here.

2.2.1 Pore flow model

In addition to a polymeric dense membrane, microporous membranes (e.g.: most inorganic ones) can also be used for gas separation. For these membranes, separation is achieved by the difference in flux between two penetrates through pores. To realize efficient gas separation, the pore radius must be nanoscale, and this number can be lower depending on the gas pairs needed to be separated. The diffusion in porous membranes is driven by the pressure drop across membrane pores, which is described by Darcy's law.

When pores size is smaller than the mean free path of gas, collisions between pore wall and gas molecules are unavoidable, which is Knudsen diffusion (**Figure 4A**). Unavoidably, bulkier gas molecules collide more times than smaller ones, and as a result, they diffuse slower. The gas flow in cylindrical pores can be given by:

$$J_i = \frac{4r\varepsilon}{3}\left(\frac{2RT}{\pi m_i}\right)^{0.5}\frac{\Box p}{lRT} \qquad (4)$$

Where m_i is the molecular weight of the penetrate, r and l are the radius and length of the pore, ε stands for the porosity of the membrane, and Δp is the pressure drop across the pore.

The selectivity can be calculated by the ratio of flow between penetrate i and j:

$$\alpha_{i/j} = (\frac{m_j}{m_i})^{0.5} \qquad (5)$$

Hence, the selectivity in Knudsen diffusion is only dependent on the molecular weight ratio of the gas pairs.

As the pore radius further decreases to a molecule level (few Å), only small molecules can diffuse through but not bulky ones. Therefore, separation based on the difference of kinetic diameter of gases is achieved, which is the molecular seizing effect [38], as shown in **Figure 4B**.

In some gas-membrane systems, surface diffusion supplements another path of permeation (**Figure 4C**) [39]. Gas molecules are adsorbed on the wall surface, and move along the pore surface and eventually diffuse through pores. Generally, the condensable species are more apt to be adsorbed than non-condensable ones. This mechanism may contribute greatly to the permeation of condensable gas, which generally is the less-permeable one through pore-flow diffusion. Hence, the competition between surface diffusion and pore flow diffusion may affect the overall selectivity [40, 41]. When the amount of penetrates adsorbed on the surface reaches a certain level, it may condense on the pore surface and block pores. In this situation, also named capillary condensation, only this type of penetrate can pass through membranes, resulting in a high selectivity.

(A) Knudsen diffusion   (B) Molecular sieving   (C) Knudsen diffusion and Surface diffusion   D) Surface diffusion & Capillary condensation
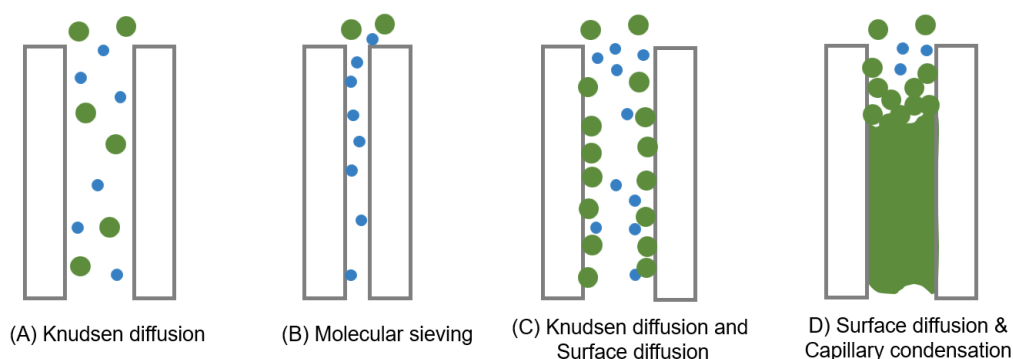
Figure 5. Scheme of A) Knudsen diffusion, B) molecular sieving effect, and C) Knudsen diffusion
incorporated with surface diffusion.

2.2.2 Solution-diffusion model

Solution-diffusion model has been proposed and described the gas transport in the polymeric dense layer since 19th century [42]. In this model, penetrate molecules firstly are absorbed by the membrane surface, and then diffuse across the membrane, which is the direction of a concentration gradient. When these molecules reach the next side of the membrane surface, desorption occurs, followed by diffusing into permeate side (as shown in **Figure 5 A**). Clearly, the penetrate transport in a polymer dense membrane is contributed by both sorption and diffusion, that is

$$P_i = D_i \times S_i \qquad (6)$$

Where P_i is the gas permeability, D_i and S_i are the diffusion coefficient and solubility of penetrate i in membranes, respectively.
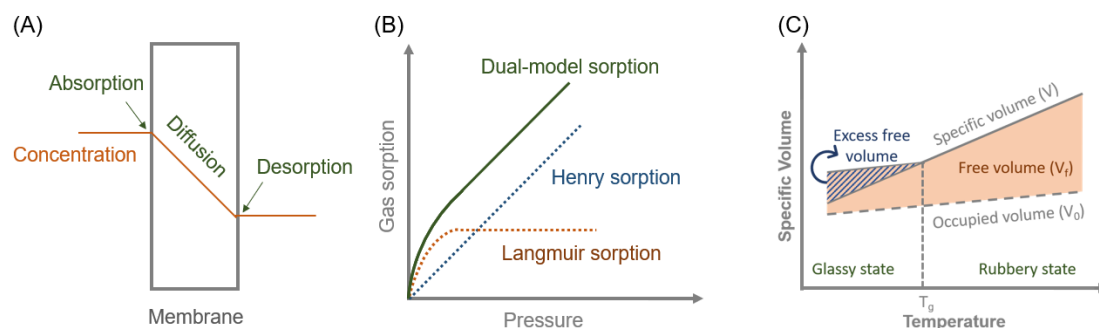
Figure 5. Scheme of (A) solution-diffusion, (B) gas sorption changes in the function of pressure, and (C) free volume of polymers in the function of temperature [43]

Solubility represents the amount of penetrates dissolved in the polymer. Several models have been historically employed to describe it, and the dual-sorption model [44](**Equation 7**) becomes the dominant one in the gas separation because of its simplicity and effectiveness in most of the cases.

$$C = k_d p + \frac{c_H b_p}{1 + c_H b_p} \qquad (7)$$

Where k_d is Henry's law coefficient, b refers to the hole affinity constant, and $c_H{'}$ stands

the saturation constant.

In this model, gas dissolves in polymers through two mechanisms: Henry's law and Langmuir sorption (**Figure 5B**). In Henry's law, polymer behaves just like ideal fluids, and penetrates simply to dissolve into their free volume sites (**Figure 5C**). There is little interaction between penetrates and polymer chains, and this normally is observed in the ideal gas-rubbery polymer system. While for glass polymers, due to the existing excess free volume, gas can also fit into these excess free volume elements, which can be approximated by Langmuir-sorption. It is worth mentioning that the dual-model is empirical rather than theoretical, and only suits gas transport in polymer dense membrane with little interaction. For other cases, the different models should be chosen wisely. For example, heavy hydrocarbons may show a convex sorption curve with increasing pressure, and in this case, the Flory-Huggins model [45] may be more suitable than the dual-model.

On the other hand, diffusivity indicates how fast penetrate transports through a membrane, and can be simply described by Fick's law of diffusion [46], which can be simply written by:

$$J_i = -D_i \frac{d\mu_i}{dx} \qquad (8)$$

Where J_i is the flux of penetrate i through membranes, and $d\mu_i/dx$ refers to the chemical potential gradient of penetrate i across a membrane. In the case of gas separation, it is generally replaced by the partial pressure gradient dp_i/dx. D_i is commonly considered as constant in an ideal system (i.e., light gas in polymer with little interaction).

Generally, in a certain polymer, the diffusivity of gases decreases with increasing kinetic diameter. While for a given gas, the diffusivity is largely dependent on the polymer free volume elements. Typically, the diffusivity of small and inert gases (e.g., H_2, He, and N_2) in a rubbery polymer is one or two orders of magnitude higher than that in a glassy polymer.

2.3 Polymeric membranes

2.3.1 Self-standing membranes

Using membranes for helium recovery has its history way back to the 1960s [30]. As natural gas from the acid gas removal step comprises approx. 90 % of nitrogen and methane **(Figure 3)**, for helium separation and recovery from natural gas, the targeted separation gas pairs are He/CH_4 and He/N_2.

Generally, the first step of developing a membrane is to investigate the intrinsic gas permeability and selectivity with a thick film (thickness typically over 100 μm). In the past few decades, the helium separation performances of a vast number of polymeric materials have been investigated. The results of membranes before 2017 have been summarized and presented in several previous review articles [35-37]. In this study, the research data from recent new studies have been collected and plotted together with the trends reported in the previous reviews in **Figure 6 (**detailed data are provided in the Supporting Information) to present the latest advances in the field. To better understand the development of membrane materials for helium separation, the widely-accepted benchmark, Robeson upper bound, was included in these figures. The 1991 and 2008 upper bound were proposed by Lloyd M. Robeson [47, 48], while the 2019 upper bound was presented by Wu et.al. [49]. These upper bounds represent the trade-off relationship between gas permeability and selectivity, revealing an intrinsic seesaw between total amount and size deviation of free volume element inside the polymeric matrix.

Generally, gas transport through polymeric membranes is based on the solution-diffusion mechanism. For the classical solution-diffusion theory, gas separation depends on the differences in gas diffusivity and solubility. However, due to the inert nature of helium, helium solubility in polymeric membranes is generally unfavorable over other gases.

On the other hand, as the kinetic diameter of helium (0.26 nm) is much smaller than N_2 (0.364 nm) and CH_4 (0.38 nm), the diffusivity differences between these gas pairs are significant, dominating in helium-favor diffusivity selectivity, and as a result, most of

the polymeric membranes are helium-selective over N_2 (as shown in **Figure 6A**). In the case of He/CH$_4$ separation, as shown in **Figure 6B**, due to the same reason, a big part of the reported membrane materials possess a He/CH$_4$ selectivity over 1. However, there are also some cases showing a He/CH$_4$ selectivity of lower than 1, indicating that the He/CH$_4$ diffusion selectivity is overcome by the loss in He/CH$_4$ sorption selectivity. These membranes are usually of rubbery polymers that favors CH$_4$ in sorption compared to helium.

As the helium content in most natural gas is very low, improving selectivity would not only reduce helium recovery cost but also enable lean-helium nature gas fields to become accessible [50]. However, due to the instinct trade-off relationship between permeability and selectivity, highly selective membranes commonly display low permeability, vice versa. *vice versa*. Some of the newly developed materials, such as polymers of intrinsic micro-porosity (PIMs) and its derivatives, present very high helium permeability (e.g., over 3000 Barrer) but with relatively low He/N$_2$ and He/CH$_4$ selectivity (mostly below 10) [51].
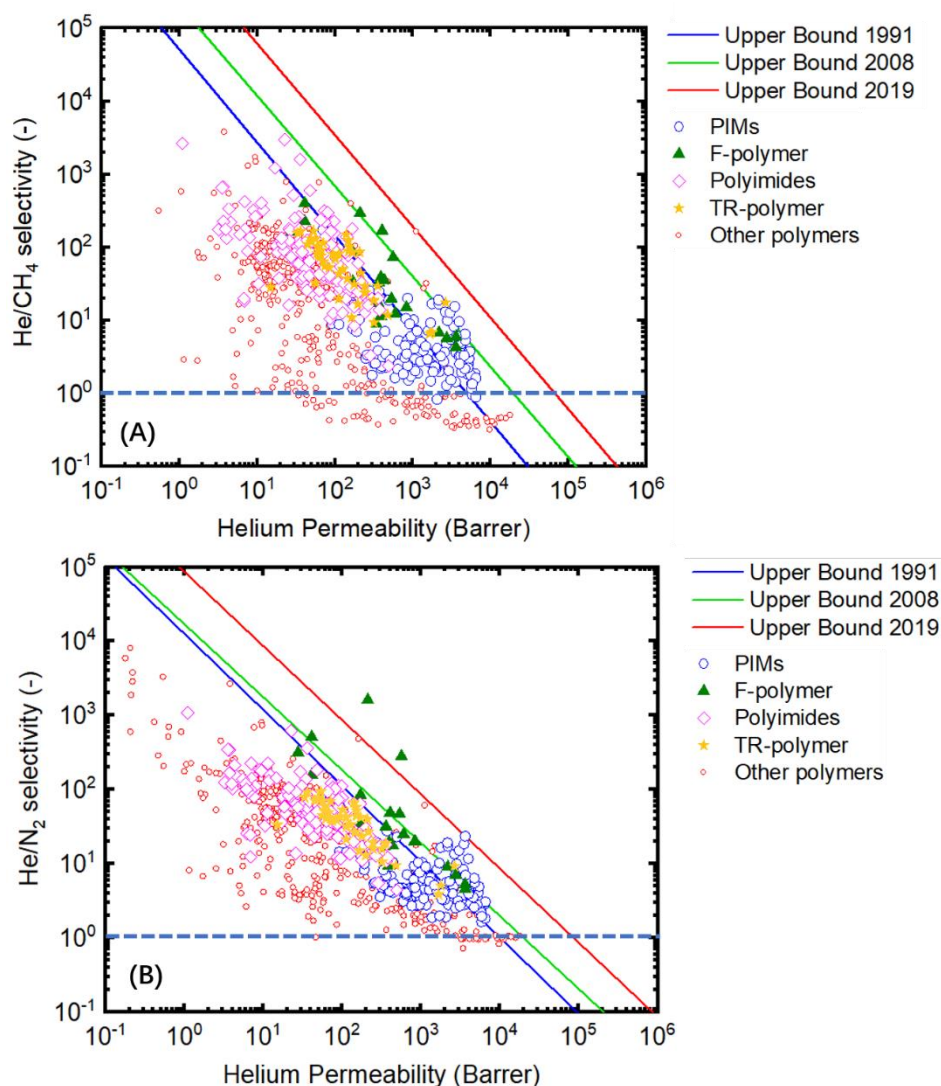
Figure 6. He/N$_2$ and He/CH$_4$ separation performances of polymeric membranes plotted with Robeson

upper bound 1991[47], 2008 [48], and a new upper bound proposed in 2019 [49].

Among the investigated polymeric materials, the perfluorinated polymer family has

shown promising helium separation performances over both N$_2$ and CH$_4$. High free

volume perfluorinated polymers, in general, exhibit ultra-high helium permeability

with moderate selectivity [52-54]. For instance, helium permeability of up to ~3000

Barrer can be obtained for homo AF and Teflon AF 2400, but the selectivity of helium

over N$_2$ and CH$_4$ usually is lower than 10 [55]. On the other hand, some perfluorinated

polymers exhibit relatively low permeability but extraordinarily high selectivity. Nafion

and Aquivion are two representative materials for this category. However, some

perfluorinated polymers show both high helium permeability and selectivity over N_2 and CH_4. For instance, a helium permeability of 560 Barrer coupled with ideal He/N_2 and He/CH_4 selectivity of 73 and 280, respectively, was obtained for poly(perfluoro-2-methylene-4-methyl-1,3-dioxolane) (Poly(PFMMD)), and helium permeability of 210 Barrer with ideal He/N_2 and He/CH_4 selectivity of 296.8 and 1615.4, respectively, was documented for poly(perfluoro-2-methylene-1,3-dioxolane) (Poly(PFMD)) [56]. Both of them have passed Robeson 2008 upper bounds for He/N_2 and He/CH_4. The combination of high permeability and high selectivity makes them up-and-coming candidates for helium separation. Nevertheless, the high-cost and complicated synthesizing processes are still main obstacles for their further industrial application. The authors believe that, if the synthesis cost can be reduced and these materials can be facilely fabricated into thin-film-composite (TFC) membranes, fluorinated polymers may become a promising candidate for helium separation.

Table 1. He separation performances of perfluorinated polymers reproduced from ref [54].

Materials	He permeability (Barrer)	Selectivity (-)		Refs
		He/N$_2$	He/CH$_4$	
Homo AF	3600	4.34	5.22	[57]
Teflon AF2400	2740	5.71	7.03	[55]
Teflon AF1600	830	15.09	20.24	[55]
Hyflon AD	340	8.95	17.00	[58]
Cytop	170	34.00	85.00	[55]
Polyperfluoropropylene	597	12.44	24.88	[59]
Poly(perfluropropyl vinyl ether)	357	17.50	31.59	[52]
Copoly(HFP-TFE)	533	19.89	46.75	[60]
Nafion	40.9	227.22	511.25	[61]
Aquivion	27.5	161.76	316.09	[62]
Polyperfluoro(2-methyl-2-ethyldioxole-1,3)	2180	6.81	9.08	[63]
Poly(PFMMD)	560	72.73	280.00	[56]
Poly(PFMD)	210	295.77	1615.38	[56]

2.3.2 Polymeric thin-film composite membranes

Despite there is a large amount of reported polymeric membrane materials, most of them are still studied in the form of self-standing thick films, with a thickness in the range of 50~100 μm. For membranes to be industrially applicable, membrane thickness

needs to be reduced to be thin, typically less than 1 μm, to ensure sufficient gas flux. In most cases, porous supports are needed in order to provide mechanical strength [31]. Fabricating TFC membranes instead of self-standing thick films is a critical step in improving the technology readiness level (TRL). Furthermore, as Baker pointed out [31], membrane permeation properties in thin membranes are different from those of their thick film counterparts. Therefore, helium separation data of TFC membranes are also collected in this work to provide more insights. Some representative data are listed in **Table 2**.

Poly(p-phenylene benzobisimidazole) (PBDI) polymeric membrane was fabricated on porous support via an interfacial polymerization process [64]. The helium permeance of ~50 GPU and ideal He/N_2 and He/CH_4 selectivity ~300 and 1000 were documented. Different from other gas pairs (e.g., CO_2/CH_4), which show strong competitive sorption, binary He/CH_4 permeation tests by varying helium contents (0-90 mol.%) at 100 ºC showed that the helium separation performance is rarely affected by the competitive transport of gases in mixed gas feeds. The membrane also exhibited good stability over a long-term of ~360 hours, making the membrane competitive with some of the perfluorinated polymers.

In another study, aromatic polyamide selective layers were coated on the top of PAN hollow fibers for helium separation [65]. The obtained TFC membranes show helium permeance of 6~8 GPU associated with the ideal selectivities of He/CH_4 and He/CO_2 in the range of 36~40 and 29~38, respectively, at 25 ºC. However, gas permeation results in mixed gas tests at the same temperature in the same study showed a sharp decrease in the He/CH_4 separation factor (in the range of 2.3~11.9, depending on stage-cut and feed pressure), implying that even though helium is a small molecule with very low solubility in polymeric matrices, competitive sorption may still negatively contribute to the selectivity. Besides, the differences in operating temperature play a role as well. Gas sorption decreases with rising temperature, and hence the influences of competitive sorption on gas transport are reduced at higher temperatures [64]. Therefore, Wang et al. [64] observed a much less significant effect of mixed feed on the

separation factor at 100 °C than the testing results at room temperature as reported by Choi et al. [65].

Dibrov et al. have fabricated asymmetric hollow-fiber membranes from commercial polyamide-imide Torlon® [66]. With a selective layer of ~ 80 nm, helium permeance of ~40 GPU and a He/CH$_4$ selectivity of 340 were obtained using 0.4 mol.% helium in CH$_4$ as feed at 35 °C. They also investigated the effect of operation pressure on helium permeance and selectivity. It was found that the transmembrane pressure has a negligible effect on both helium permeance and He/CH$_4$ selectivity when it is lower than 60 bar. However, when the transmembrane pressure was above 70 bar, a significant decrease was observed for both permeance and selectivity, possibly due to the collapsing of pores with a diameter smaller than 15 nm in the hollow fiber and the accelerated physical aging of selective layer under high-pressure conditions.

Teplyakov and coworkers functionalized Matrimid® 5218 asymmetric hollow fibers with a direct gas-phase fluorination process [67]. They found out that fluorination can be an effective method to enhance the He/CH$_4$ selectivity. For instance, modifying the Matrimid 5218 membrane module with a He/F$_2$ mixture containing 2 vol.% of F$_2$ resulted in an ideal He/CH$_4$ selectivity of ~800, while the unmodified module showed an idea He/CH$_4$ selectivity of only 146. It is worth mentioning that He flux of the membrane module showed nearly unchanged after fluorination. Increasing F$_2$ content in the modification gas stream to 10 vol.% has led to higher selectivity of ~8000 but also a higher degradation rate over time. Hence, the fluorination process parameter should be precisely optimized. The authors also investigated the long-term stability of the hollow fiber membranes in a time frame of up to 10 years. It was found that the permeances of both helium and CH$_4$ decrease over time, while the reduction rate for CH$_4$ was much faster, resulted in an enhanced He/CH$_4$ selectivity. For example, 55 % of the initial helium permeance was lost (from 83 to 37 GPU) in 10 years, but the He/CH$_4$ separation factor increased from 146 to 4460.

Table 2. Permeance and selectivity of selected membranes for He/CH$_4$ and He/N$_2$ separation.

Membrane materials	He permeance (GPU)	Selectivity (-)	Refs

|		He/CH$_4$	He/N$_2$	
CA	106	31	34	[68]
Poly(p-phenylene benzobisimidazole) (PBDI)	~50	100	~300	[64]
Aomatic polyamide	6~8	36~40	--	[65]
Torlon®	~40	340	--	[66]
Fluorinated Matrimid® 5218	80~183	200~8000		[67]
PIM-1	190 ± 40	~12	~15	[69]

To sum up, most reported polymeric membrane materials present low helium separation performances below the upper bound proposed in 2008. For membranes giving helium permeability of higher than 1000 Barrer, the He/N$_2$ selectivity is usually lower than 10. In idea case, adding nanofillers such as porous nanomaterials (e.g., zeolite, metal-organic frameworks (MOFs)) with a molecular sieving effect into these materials can enhance the selectivity while maintains the high gas permeability. While other membrane materials exhibit He/N$_2$ or He/CH$_4$ selectivity over 100, the helium permeability usually is lower than 100 Barrer. Fabrication of asymmetric membranes or TFC membranes with a thinner selective layer may improve gas permeance. But it is of great importance to ensure that those membrane materials could maintain similar separation properties compared with their thick-film counterparts.

2.4 Carbon molecular sieve (CMS) membranes

CMS membranes are promising membrane materials for helium separation. As can be seen from its name, CMS membranes generally separate gas molecules based on the molecular sieving mechanism, i.e., smaller gas molecules pass through while larger species are retained. Hence, it could offer high selectivity if the pore size can be appropriately selected/designed by controlling the pyrolyzing conditions (e.g., heating rate, pyrolyzing temperature, and pyrolyzing atmosphere) for specified gas pairs [70]. CMS membranes have been widely studied for H$_2$ separation over other bulky gases (e.g., CO$_2$, CH$_4$) due to high H$_2$ selectivity over gases caused by great differences in their kinetic diameters [71-73]. CMS membranes have been also applied for helium separation as early as the 1970s [74], since then, several polymers such as polyimide, cellulose, poly(phenylene oxide) have been used as precursors for CMS membrane fabrication for helium separation [75]. However, since H$_2$ separation has obtained much

more attention than He separation, CMS-related studies have been focused on H_2 separation rather than helium separation in the past decades. Considered H_2 and helium are rather similar in kinetic diameters and their inert chemical properties, the experience and knowledge from H_2 separation membrane should be greatly helpful guideline for He separation membrane development in the future [71].

The pore property, and hence the membrane separation performances of CMS membranes, depends primarily on carbonization temperatures, precursor types, and carbonization gas atmospheres. As presented in **Table 3** and **Figure 7**, when carbonization temperature increases, helium permeability of carbon membranes gradually decrease with improvement in both He/N_2 and He/CH_4 selectivity. For instance, for the CMS membranes fabricated from a PIM-PI [76], except for the one carbonized at 550 ℃, most samples exhibited a clear trend moving towards the upper left side for both He/N_2 and He/CH_4 separations. Besides, between 600 to 700 ℃, there is a significant increase in both He/N_2 and He/CH_4 selectivity with only a moderate loss in helium permeability. It is expected that the increase of the final carbonization temperature leads to the formation of a more ordered graphitic structure and smaller pores, which enhances the helium selectivity based on the molecular sieving mechanism with fewer defects [77]. However, further increasing the pyrolysis temperature leads to only a slight increment in selectivity but a considerable sacrifice in gas permeability due to the decreased porosity with the surface sintering effect. Therefore, pyrolysis conditions should be carefully designed and optimized as it plays a crucial role in turning the pore structures and separation performance of the final CMS membranes.
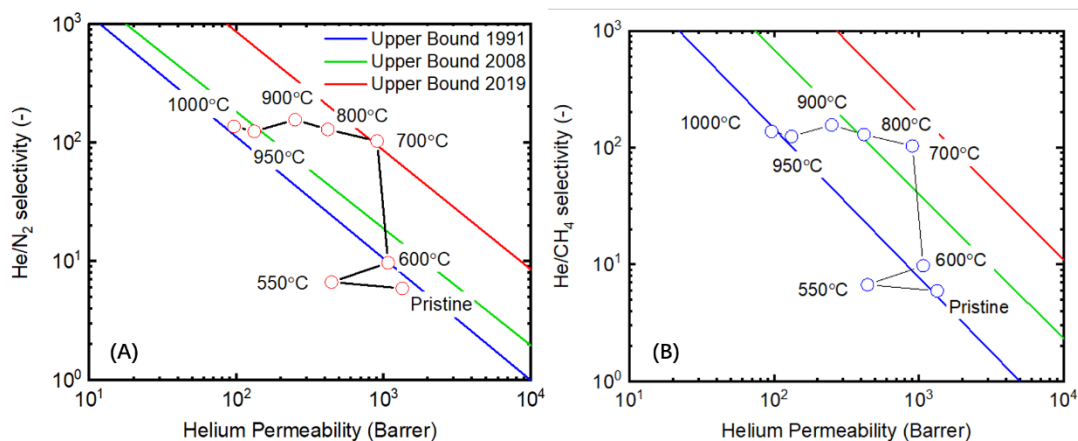
Figure 7. Effect of pyrolysis temperature on He/N$_2$ (A) and He/CH$_4$ (B) separation performances (data

source from [76])

Table 3. Helium separation performances of carbon membranes

Precursor materials	Pyrolysis conditions	Helium permeability (Barrer)	Ideal selectivity (-)		Refs
			He/CH$_4$	He/N$_2$	
PI/PVP	550	1691.17	--	36.06	[78]
	550 PI10	2035.75	--	36.06	[78]
	550 PI40	2527.46	--	29.05	[78]
	550 PI55	2816.21	--	25.67	[78]
	700	1064.66	--	118.80	[78]
	700 PI10	1433.71	--	111.59	[78]
	700 PI40	1550.52	--	91.03	[78]
	700 PI55	1785.26	--	88.22	[78]
Matrimid and Kapton	NMP, 475 °C	18.24	49.28	22.80	[79]
	NMP, 650 °C	65.59	33.76	27.14	[79]
	γ-butyrolactone, 475 °C	21.41	30.05	30.05	[79]
	γ-butyrolactone, 450 °C	8.69	58.67	58.67	[79]
	Allotherm, NMP 550 °C	154.69	26.75	15.62	[79]
PIM-PI	Pristine	1340.00	4.11	5.93	[76]
	550 °C	442.00	6.14	6.70	[76]
	600 °C	1073.00	13.85	9.75	[76]
	700 °C	903.00	158.42	103.20	[76]
	800 °C	418.00	449.46	129.41	[76]
	900 °C	250.00	925.93	156.25	[76]
	950 °C	132.00	1269.23	124.53	[76]
	1000 °C	96.00	4800.00	137.14	[76]
	1000 °C after 250 days	78.00	6000.00	162.50	[76]
PIM-PI	pristine	316.75	2.07	4.94	[80]
	500 °C	307.64	10.66	12.73	[80]
	550 °C	387.18	10.25	18.89	[80]
	600 °C	303.55	15.20	12.48	[80]

	650 °C	114.78	11.31	7.93	[80]
	700 °C	66.92	17.11	11.31	[80]
	750 °C	146.36	82.91	55.88	[80]
	800 °C	90.58	231.22	84.56	[80]
BPDA-pPDA		145.63	--	3.77	[81]
Branched PEI	550 °C, 30 min	700	--	11.67	[81]
Cellulose	550 °C	126	--	788	[82]
	600 °C	174	--	1993	[82]
	600 °C	403	~4000	~400	[83]
poly(vinylidene chloride)	1000 °C, test temp -15 °C	280	--	--	[84]
	0 °C	340	--	--	[84]
	25 °C	440	--	--	[84]
PI/SiO₂	SiO$_2$-10	1100	61.11	27.50	[85]
	SiO$_2$-20	1930	45.95	26.81	[85]
	SiO$_2$-30	5350	31.47	25.48	[85]
	SiO$_2$-20, DMDES/TEOS ratio 0.25	2110	35.17	25.42	[85]
	SiO$_2$-20, DMDES/TEOS ratio 0.5	6300	26.25	25.20	[85]

In addition to the polymers as mentioned above, several natural materials, like cellulose, have been employed as precursors and reported promising progress for helium separation application. Mendes and co-workers developed CMS membranes using natural cellulose as a precursor [82]. In their report, a hybrid solvent composing of dimethyl sulfoxide and 1-Ethyl-3-methylimidazolium acetate ([Emim][Ac]) was chosen to dissolve cellulose, and the flat-sheet cellulose membrane was obtained by phase inversion. The obtained membrane was pyrolyzed at a temperature of 550 °C or 600 °C. The CMS membranes formed at 600 °C displayed a remarkably high He/N$_2$ ideal selectivity of 1993 with a helium permeability of 174 Barrer, really close to 2019 upper bound. In addition to dry conditions, the authors have investigated the permeance stability of these CMS membranes in humid conditions. Generally, moisture is prone to be absorbed by the pores inside CMS membranes and then inhibits other gas transport. However, in this work, humid tests (75-77 % relative humidity) showed a sharp increase in both O$_2$ and N$_2$ permeability, but N$_2$ permeability was more significantly enhanced (c.a., 9-times), thus resulted in O$_2$/N$_2$ selectivity decreasing from 24 to 7. Even though

helium permeability was not tested under humid conditions, a similar situation is expected. These surprising results can be rationalized by the hydrophilicity of cellulose-based CMS. Recently, Lei et al. reported the cellulose-based carbon hollow fiber membranes (CHFMs) and presented a high helium permeability of 403 Barrer with a He/CH$_4$ selectivity of > 4000 [83], showing great potential for helium recovery from natural gas.

Most of the CMS membranes were obtained by the carbonization of neat glassy polymers. It is also worth mentioning that Park et al. developed a series of CMS membranes using SiO$_2$-functionalized polyimide as precursors [85]. By varying SiO$_2$ amount and polyimide types, CMS membranes with a helium permeability of up to 6300 Barrer were obtained with moderate ideal He/CH$_4$ selectivity. It suggests a new methodology of incorporating porous fillers into CMS matrices to improve gas permeability and selectivity.

Helium separation performances of CMS membranes were plotted in Robeson upper bounds (shown in **Figure 8**). Compared to polymeric membranes, helium separation peroformances of CMS membranes are rather promising. Several CMS membrane materials exchibited a both He/CH$_4$ and He/N$_2$ separation performances cross-over the upper bound 2019. However, compared to polymeric membranes, there are only limited reports about using CMS membranes for helium separation. Developing CMS membranes for helium separation, specially from cheap and substainable procusors, can be a interesting topic.
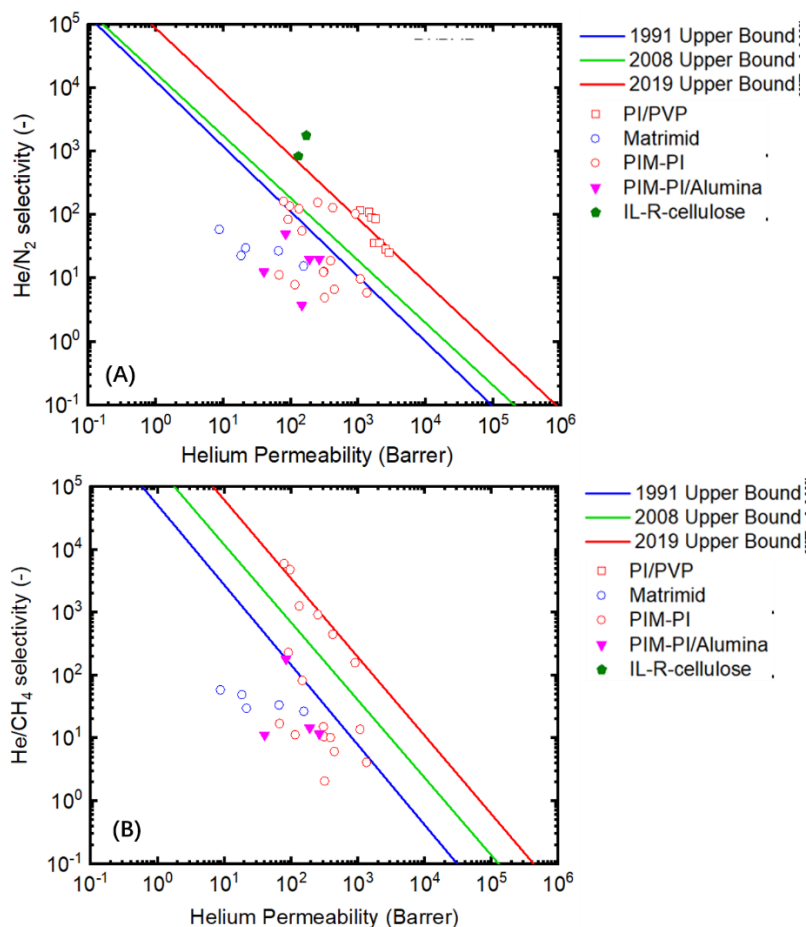
Figure 8. He separation performances of carbon membranes plotted in Robeson upper bound [48] and the upper bound proposed in 2019 [49].

Other than thick CMS films, research work has been also carried out on fabricating asymmetric self-supported CMS membranes and supported CMS membranes for helium separation. Some of the representative results have been summarized in **Table 4**.

Table 4. Asymmetric and supported CMS membranes for helium separation

Precursor materials	Pyrolysis/Test conditions	He permeance (GPU)	Selectivity (-)		Refs
			He/CH$_4$	He/N$_2$	
P84	Precursor	33.4	4.99	6.30	[86]
	900 ºC, 5 min	3.53	415.29	353.00	[86]
	900 ºC, 30 min	3.08	603.92	342.22	[86]
	900 ºC, 60 min	2.34	2925.00	320.55	[86]
P84	900 ºC, 5 min, test temp 40 ºC	2.9	408.45	446.15	[87]
	test temp 60 ºC	3.53	415.29	353.00	[87]
	test temp 100 ºC	4.61	475.26	230.50	[87]

P84	600 ºC	70.03	20.94	16.93	[88]
	700 ºC	186.30	16.93	9.95	[88]
	800 ºC	235.41	4.25	3.58	[88]
	900 ºC	409.27	5.48	3.15	[88]
P84	800 °C, 15 min	704.76	--	268.99	[89]
	800 °C, 30 min	821.98	--	296.74	[89]
	800 °C, 45 min	984.92	--	305.88	[89]
	800 °C, 60 min	795.66	--	278.20	[89]
P84-NCC	800 ºC, 1ºC/min	1271	--	408.68	[90]
	800 ºC, 3ºC/min	1493	--	463.66	[90]
	800 ºC, 5 ºC/min	1057	--	343.18	[90]
	800 ºC, 7 ºC/min	1018	--	338.21	[90]
P84-NCC	600 ºC	568.93	--	293.26	[91]
	700 ºC	1003.42	--	359.65	[91]
	800 ºC	1493.62	--	463.86	[91]
	900 ºC	1297.66	--	452.15	[91]
P84/NCC	800 °C, 30 min	1493.62	--	463.86	[92]
P84/NCC-AL	800 °C, 30 min	1459.21	--	475.31	[92]
P84/NCC-C	800 °C, 30 min	1386.42	--	460.61	[92]
P84/NCC-CMS	800 °C, 30 min	1402.11	--	461.22	[92]
Kapton	Ar, 600 ºC	150.20	8.49	6.64	[93]
	N_2, 600 ºC	258.62	14.61	9.57	[93]
	He, 600 ºC	276.30	15.61	8.78	[93]
	Vacuum, 600 ºC	305.07	17.24	8.50	[93]
Kapton	700 °C, CO_2 partial pressure 15 kPa	283.52	37.80	354.97	[94]
	700 °C, CO_2 partial pressure 75 kPa	222.16	40.14	370.60	[94]
	700 °C, CO_2 partial pressure 250 kPa	175.57	30.23	407.15	[94]
Organosolve-lignin, and a phenol resin	OrL-773	20.03	21.01	11.99	[95]
	OrL-Fe-773	24.80	366.27	182.89	[95]
	Orl-873	4.61	136.32	136.32	[95]
	OrL-973	0.54	320.48	110.09	[95]
	BP-773	24.74	5.66	7.03	[95]
	BP-Fe-773	16.04	36.70	21.94	[95]
Resorcinol–formaldehyde resin	CMSM 500	350	--	221	[96]
	CMSM 550	420	--	>544.0	[96]
Phenolic resin	600 ºC	501.21	1.73	1.64	[97]
	700 ºC	550.72	2.73	1.93	[97]
	800 ºC	152.17	63.00	137.30	[97]
	900 ºC	75	--	24.4	[97]
Sulfonated phenolic resin	III-1 precursor	3.71	118.45	156.62	[98]
	III-1	4.91	124.62	156.62	[98]
	III-2	163.39	837.13	253.75	[98]
	IV-1 precursor	239.15	187.09	96.67	[98]
	IV-1	539.04	201.90	87.33	[98]
	IV-2	581.71	41.81	31.62	[98]
	IV-3	895.79	30.06	19.03	[98]

Nanographite	Test temp, 22 °C	0.13	--	--	[99]
	Test temp, 74.59 °C	0.39	--	--	[99]
	Test temp, 102.31 °C	0.67	--	--	[99]
	Test temp, 125.14 °C	0.97	--	--	[99]
	Test temp, 152.85 °C	1.21	--	--	[99]
PIM-PI/alumina	precursor	40.01	11.23	12.64	[100]
	500	188.90	14.55	19.87	[100]
	600	262.96	11.69	19.95	[100]
	700	83.69	180.75	49.88	[100]
Metal oxide/PIM-PI	500 °C	316.23	11.29	11.29	[101]
PPO on ceramic support	500 °C	165.56	85.32	34.09	[102]
	600 °C	716.11	326.14	172.80	[102]
	700 °C	146.33	52.98	28.07	[102]
	800 °C	204.61	268.61	125.78	[102]
PVDC–PVC	500 °C	8.70	13.08	10.06	[103]
	600 °C	29.22	27.49	16.44	[103]
	700 °C	38.01	27.81	11.40	[103]
CNT	--	206.91	--	2.16	[104]
PEI	600 °C, 30 min	2020	--	24	[105]
--		~375	--	~100	[106]

P84, a co-polyimide licensed by Evonik [107], is a thermally stable co-polyimide of 3,3'4,4'-benzophenone tetracarboxylic dianhydride with 80% methylphenylene-diamine + 20% methylene diamine (chemical structure shown in **Figure 9**). It has been intensively studied as precursors for CMS fabrication due to its relatively low cost and superior mechanical strength.
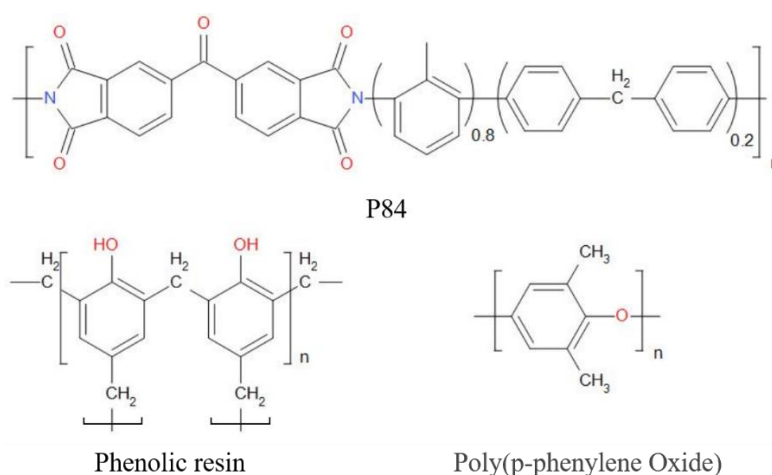
Figure 9. Chemical structure of P84 polyimide, phenolic resin and poly(p-phenylene oxide).

The different operation parameters during carbonization have been systematically

investigated for the preparation of P84-based CMS membranes. However, various research groups obtained quite different results, as shown in **Table 4**. For instance, both Favvas et al. [86] and Barsema et al. [88] reported asymmetric carbon hollow fiber membranes fabricated from P84 with the pyrolysis temperature of 900 °C for 1 h. Favvas and co-workers observed the helium permeance of 2.34 GPU at the testing temperature of 60 °C with a He/N_2 and He/CH_4 ideal selectivity of 320 and 2925, respectively, [86]. On the other hand, the CMS membranes fabricated by Barsema et al. displayed almost 20-fold higher helium permeance (~ 400 GPU) with much lower He/CH_4 and He/N_2 selectivities (3-5.5) at 25 °C [88]. In another study reported by Mohamed et al., both high helium permeance (984.92 GPU) and high He/N_2 selectivity (305.9) were obtained at room temperature [89]. It is worth noting that the pyrolysis temperature (800 °C) in that work was lower than the previous two studies. Despite the discrepancy in testing temperature and pyrolysis conditions, this significantly distinct performance should be treated with more attention.

Compared to the CMS fabricated from neat P84, CMS prepared from P84-based MMMs showed better helium separation performances. Sazali et al. have chosen cellulose nanocrystal (NCC) as fillers blending with P84 as precursors for CMS tubular membranes [90-92, 108]. The introduction of NCC decreased the MMM's thermal stability and thus reduced the carbonization temperature. In these studies, various parameters were investigated, including pyrolysis temperature [91], NCC content, stabilization temperature [108], the presence of an intermediate layer, and intermediate layer type [92]. Among them, the most influential parameter is the final pyrolysis temperature (3-time and around 60% increments in helium permeance and He/N_2 selectivity, respectively). Moreover, increasing NCC contents from 5 to 9 wt% firstly increased helium permeance by 7% and then decreased to the original value, while He/N_2 selectivity kept almost unchanged and then decreased at 9 wt% NCC amount. The presence of intermediate layer between tubular support and CMS layer increases the mass transport resistance and hence decreases the gas permeation flux, and the changes were related to the intermediate layer type (up to 7 % loss in flux). However,

both factors have little influences on He/N$_2$ selectivity. Furthermore, it is found out that stabilization temperature could also significantly contribute to the final separation performances [108]. Increasing stabilization temperature from 250 to 450 °C resulted in a sharp decrease in helium permeance (from 1027 GPU to 736 GPU), while the He/N$_2$ selectivity firstly increased to 432 and then decreased to 344.

Kapton, another commercial polyimide, has also been applied in CMS fabrication for helium separation. By changing the carbonization atmosphere (vacuum, argon, helium, and nitrogen), helium permeance can be tuning from ~150 to ~300 GPU, with an order of vacuum < nitrogen < helium < argon. This result denotes that the gas atmosphere also needs to be taken into consideration for CMS membrane preparation [93]. In another study, the CMS with Kapton as precursor presented the feed-pressure sensitive phenomena: for all the gases tested, increasing feed pressure from 15 to 250 kPa resulted in a significant reduction in permeance (25 – 50%) [94]. Interestingly, the loss in helium permeability is larger than that in N$_2$ but lower than in CH$_4$. Hence the selectivity of He/CH$_4$ increased while that of He/N$_2$ decreased.

Resins with different chemical structures are another precursors for CMS fabrication [98]. CMS based on resins normally presents higher selectivity but lower helium permeability than CMS fabricated via polyimides [95]. However, by functionalizing the resin with different groups, helium permeance of up to 163.4 GPU combined with He/CH$_4$ and He/N$_2$ selectivity of up to 837.1 and 253.8, respectively, can be obtained[98].

Highly permeable PIM-PI has been employed to fabricate TFC CMS on alumina support [100]. Even though the selective layer of the supported CMS membrane is very thin (< 100 nm), its overall helium permeance is located in a moderate region. In addition, the fabricated CMS membranes face a serious physical aging problem: in a period of ~50 days, the permeance of all the tested gases reduced significantly. For instance, the 82 nm CMS pyrolyzed at 600 °C lost 88% helium permeance with more than 95 % reduction for N$_2$ and CH$_4$ after 50 days, which makes these membranes impractical for any gas separations. This CMS membrane was further modified by in-

situ introducing Al_2O_3 nanoparticles into the cast membrane solution using vapor phase infiltration [101]. After carbonization, an extra PDMS layer was coated on the CMS membranes as a protective layer. The presence of Al_2O_3 nanoparticles indeed enhanced gas permeance but declined gas selectivity. But more importantly, the aging rate was slower compared to CMS derived by neat PIM-PI precursors.

Except for the precursors mentioned above, other polymeric materials have also been investigated for CMS membranes, including PPO [102], PVDC–PVC [103], and PEI [105]. Many of them are cast on inorganic substrates as TFC on a small laboratory scale. Different from the aforementioned lab-scale reports, Parsley et al. developed full-scale CMS membrane modules with 86 tubes and tested them in real coal- and biomass-derived syngas [106]. This membrane was originally designed to purify hydrogen from syngas, where helium was used to investigate long-term stability. Results show that both helium and N_2 permeances were stable throughout the ~330 h continuous test. Besides, the field test (syngas) results were comparable to the value obtained from lab-scale tests in terms of selectivities, stage-cuts, and the hydrogen retentate concentrations. Considered the similarity of helium and H_2 transport inside membranes, this work demonstrates that CMS membranes initially designed for H_2 separation may be also promising for helium separation.
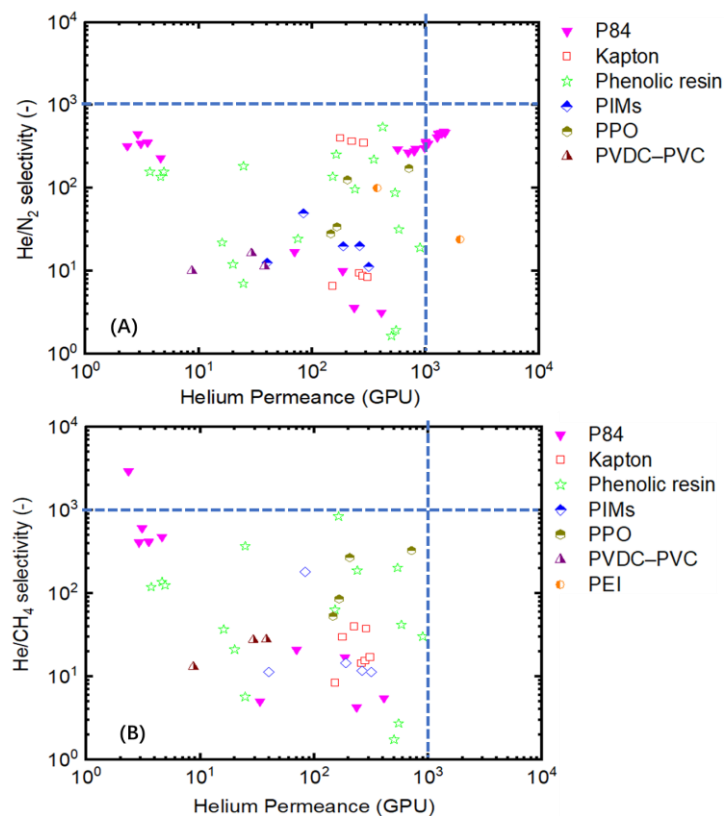
**Figure 10.** Carbon asymmetric or supported membranes for He separation.

The He/N_2 and He/CH_4 separation performances of asymmetric CMS membranes were also summarized in **Figure 10**. As it can be seen, for both He/N_2 and He/CH_4 cases, helium permeance of 1000 GPU and selectivity of 1000 (selectivity obtained from H_2/N_2 and H_2/CH_4 gas pairs) seem to be an upper limit for CMS membranes, as most reported permeation data are below this limit.

To sum up, although most of the current CMS membranes were intendedly developed for hydrogen purification or CO_2/CH_4 separation, these CMS membranes exhibit exciting He separation performance. Some of them have been located on the benchmark upper bound lines. However, more efforts should be devoted to developing CMS membranes with superior helium separation properties. At the same time, reducing the physical aging of CMS is another critical issue that needs to be addressed. Thirdly, the long-term stability of carbon membranes when exposed to impurities in feed gases should be considered to reduce membrane regeneration costs and increase membrane lifetime.

2.5 Porous inorganic membranes

Inorganic membranes (e.g., silica, zeolite) have been investigated for helium separation since 1980s [109, 110]. Inorganic membranes hold several advantages over polymeric membranes, such as no swelling and compaction, good stability in harsh conditions, like high temperatures and corrosive environments [73]. Therefore, even though it is commonly accepted that the fabrication of inorganic membranes is complicated, and the costs are normally high compared with polymeric membranes, inorganic membranes still find applications in many fields (e.g., water purification, gas separation).

For most porous inorganic membranes, gas separation is achieved by molecular sieving. Therefore, separation depends directly on their pore sizes. If the pore sizes are larger than the range where molecular sieving may apply, Knudsen diffusion and capillary condensation may occur, resulting in little or no selectivity. A thorough review of the fundamentals of inorganic membranes and their helium separation performances was published in 2017 [35]. Thus, this section will skip the fundamentals of inorganic membranes (e.g., material selection, fabrication, separation mechanism) and only focus on summarizing and analyzing the helium separation data. Similar to previous sections, the helium separation results were plotted and compared with the upper bound proposed in 1991, 2008, and 2019 as shown in **Figure 11**.
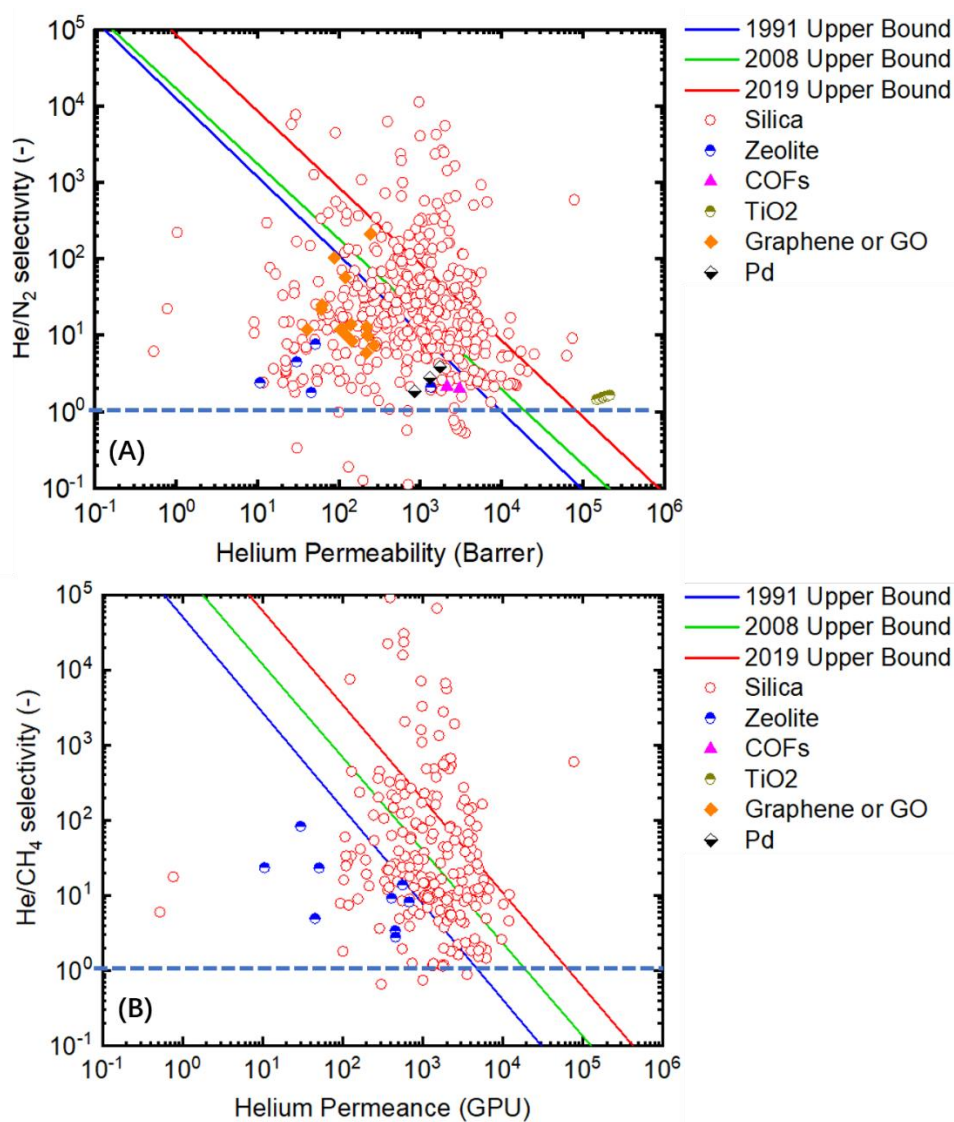
Figure 11. Inorganic membrane He/N$_2$ and He/CH$_4$ separation performances

2.5.1 Silica membranes

Silica membranes were firstly discovered in the early 1980s [111, 112]. Since then, silica membranes have been intensively studied for various applications, including gas separation [113], liquid purification [114], and pervaporation [115]. Silica membranes have been investigated for helium separation since that [109, 110].

As can be seen from **Figure 11**, compared to polymeric membranes, many silica membranes exhibited extraordinarily high helium permeance and selectivity over other gases, making their separation performances far surpass the upper bounds [35].

Although the silica membranes are considered to present excellent separation performances at high temperature and high-pressure conditions, the stability has been reported to be vulnerable to water vapor. Duke et al. observed a continuous decline in gas permeance within the first few hours of testing with the presence of 34 mol.% steam, and losses of around 50% or greater in permeance were documented in 60 h [116]. Further removal of steam cannot completely recover the gas permeance, and it was ascribed by the water-induced pore collapsing inside silica membranes. In another study, Asaeda et al. found that after exposure to humid gases over four months, the H_2 permeance of the silica membrane reduced to 1/10 of the original value [117].

Different methods have been developed to improve the stability of silica membranes, and surface hydrophobicity enhancement is one of the most commonly employed methods. However, this method usually leads to lower selectivity. Doping the silica with other metal ions and designing new precursors [118] in the membrane fabrication process have been proven to be effective in improving the thermal stability of silica membranes [119].

Generally, state-of-the-art silica membranes typically consist of a thin silica layer on top of mesoporous support, which provides mechanical strength. Surprisingly, Gu et al found out that applying an intermediate layer of γ-alumina between the porous support and the selective layer could also effectively reduce the transport resistance to water vapor and improve the hydro-thermal stability [120].

Overall, even though significant progress has been made in silica membrane fabrication, the poor reproducibility, which results in large fluctuations in performance and often poor separation properties, is still the fundamental problem limiting the industrial application of silica membranes [113].

2.5.2 Zeolite membranes

Zeolites have been widely studied as membrane materials due to their unique advantages, including uniform pores with molecule-size dimensions, high porosity, and excellent thermal and chemical stability [121]. Many different types of zeolite

membranes have been developed, such as LTA [122], FAU [123], MOR [124], FER [125], MEL [126, 127], CHA [128, 129], SAPO-34 [130, 131], DDR [132], and AFI [133]. There are several review articles about zeolite membrane fabrication, separation mechanism, and applications [121, 134, 135]. The interested reader could find more details about state-of-the-art techniques, concepts, and achievements in this field via the above-mentioned references.

Compared to silica membranes, there are not many zeolite membranes reported for helium separation. Some of them were listed in ref [35]. The results reveal that zeolite membranes typically display He/N_2 selectivity of lower than 10.

For He/H_2 separation, although different membranes show significant differences in helium permeances (varying from around 1500 GPU (i.e., ~ 1500 Barrer in terms of permeability) [136] to greater than 26000 GPU (i.e., ~ 14300 Barrer in terms of permeability) [137]), their selectivities are usually located in the same range of 2~3 or lower, denoting that the pore size of zeolite membranes are too big for helium separation. Antunes et al. also carried out the test of MFI-ZSM-5 zeolite-type membranes for the separation of hydrogen isotopologues from helium [138]. In the whole tested temperature range (25-125 °C), the membrane exhibited a faster transport rate for H_2 or D_2 than He, resulting in the selectivity of H_2/He and D_2/He of ~1.8 and 1.2, only slightly higher than the typical Knudsen diffusion selectivity.

In another study, SAPO-34 zeolite membranes have been applied for He/CH_4 separation [139]. By using the equimolar He/CH_4 mixture as the feed gas, the SAPO-34 membranes displayed helium permeance of around 560 GPU (i.e., ~ 4368 Barrer in permeability) and He/CH_4 selectivity of 13.8. Considering the thickness of the fabricated membranes is around 10 μm, if the membrane thickness can be reduced to lower than 1 μm, this membrane can be a competitive candidate for He/CH_4 separation. CHA zeolite-based membranes have also been reported for helium separation [140]. For a single gas permeation test carried out at 200 °C, ideal He/N_2 and He/CH_4 selectivity of 1.8 and ~5, respectively, were obtained with helium permeance of ~45 GPU (i.e., ~ 265 Barrer in permeability).

DDR type zeolite membrane with an aperture of 0.36×0.44 nm was formed on a porous alumina substrate and used for helium separation by Tomita et al [141]. They found that when test temperature increased from 25 to 100 ºC, helium permeance and helium selectivity over N_2 and CH_4 were both enhanced. Later on, helium permeance of ~ 30 GPU, and He/N_2 and He/CH_4 selectivity of 4.5 and 83.3 of a DDR membrane with a 5-10 µm selective layer were also documented at 100 ºC [141], indicating that such membrane becomes more competitive with increasing temperature. DDR-3 type zeolite membrane prepared by Wang et al. [142] was intentionally for separating Xenon from CO_2, while helium permeance was also investigated using single gas permeation tests. Helium permanence of ~50 GPU (i.e., ~ 220 Barrer), coupled with He/N_2 and He/CH_4 selectivity of 7.7 and 23.3, respectively, were documented.

Compared to silica membranes, zeolite membranes hold advantages of relatively easier preparation, the possibility to modify their chemical compositions via cation exchange (thus possibly change the aperture size). But overall, zeolite membranes generally present a relatively low helium selectivity over N_2 and CH_4, making zeolite membranes less attractive than silica membranes for helium separation.

2.5.3 Emerging inorganic membranes

Other than the above-mentioned silica and zeolite membranes, emerging inorganic membranes have become a highlight in the recent year thanks to the appearing novel nano-materials. A great number of new membranes have been studied for helium separation, including MOF membranes [143-145], graphene or graphene oxide (GO) membranes [146], covalent organic framework (COF) membranes [147, 148], and other inorganic membranes [149, 150].

MOFs' pore aperture and pore size can be tuned by selectively choosing organic linkers with proper length and functional groups. By adjusting the combination of organic linkers and metal ions, more than 100,000 types of MOFs can be made, according to the literature [151]. MOF membranes are promising for improving membrane performances by taking advantage of MOFs' highly designable properties, high

porosity, and sharp pore size distributions. MOF membranes have been intensively studied in recent year for various gas separation applications including CO_2/CH_4 [152, 153], CO_2/H_2 [154, 155], CO_2/N_2 [156, 157], paraffin/olefin [158, 159] and helium separations [160-162]. Despite the different organic linkers and metal ions employed in MOFs preparation, the reported MOF membranes generally showed a low He/CH_4 selectivity of only 1~2 and He/N_2 selectivity of 3~4 [145, 160-162]. It is possibly caused by the non-selective voids between MOFs crystals, where all gasses quickly pass through, resulting in these low selectivities. To address this issue, Cehn et al. fabricated ZIF-8 membranes forming by large single crystals, and gas permeation properties of the resulted membranes were tested [143]. The single-crystal membranes without grain boundaries exhibited a He/CH_4 selectivity of up to 40.1 and He/N_2 selectivity of 144.4, which represent the highest values of current MOF membranes. However, considering the size of a single crystal is in the range of micrometers (~ 400 μm), upscaling of this type of membrane can be quite challenging.

Graphene- and GO- incorporated materials have been a hot research topic in the membrane separation field in the past few years [163, 164]. Membranes based on these two materials and their derivatives have been widely applied in liquid purification and gas separation [165, 166]. Gestel et al. developed GO membranes by dip-coating a GO dispersion on a specially designed ZrO_2 (8YSZ type) mesoporous support, followed by a thermal treatment in air at 300 °C for 1 h [167]. Further thermal treatment at 750 °C for 1 h in an atmosphere of 3% H_2 and 97% Ar was employed to reduce GO membranes into graphene membranes. The obtained graphene membranes (GO layer: 5-10 nm thick) showed higher helium permeance and selectivity over CH_4 and N_2 compared with GO membranes. Under optimized operation conditions, helium permeance of 239 GPU and He/N_2 selectivity of 215 were documented at 200 ºC and transmembrane pressure of 4 bar. Zhu et al. also developed a composite GO membrane on YSZ ceramic hollow fibers [168], in which the selective layer's thickness was down to 230 nm, while a helium permeance of ~120 GPU was documented associated with a He/N_2 selectivity of 58. It is also noticeable that the membrane showed a good long-term stability (around 240 h)

in H_2/N_2 separation at the room temperature.

In another report, Nezhad et al. developed a graphene membrane by compressing the 2D graphene by high pressure [169]. Even though the fabricated membrane has a thickness in millimeter range, most of the obtained helium permeance is in the range of 100~200 GPU, accompanied by a He/N_2 selectivity of 10~20. Attempts were also made to incorporate a second layer of graphene/zeolite, while no apparent changes can be found for both He permeance and He/N_2 selectivity.

Li et al. developed a 2D layered COF membrane for helium separation [147], where the 2D COF-1 nanosheets were exfoliated from their bulky state and then coated on hollow fiber support. Gas permeation tests were carried out from room temperature to 400 °C. Helium permeance of up to 3000 GPU was documented but with a He/N_2 selectivity of only ~2, demonstrating that the pore size of the used COF-1 (~0.6 nm) was too big for helium separation. It is worth mentioning that the COF membrane exhibited superior thermal stability: a long-term single-gas permeation was carried out at 350 °C, and the membrane showed almost no decline in H_2, N_2, and SF_6 permeance for 30 h.

Palladium is famous for its the almost infinite hydrogen selectivity over other gases and hence has been employed for hydrogen separation for decades, especially at high temperatures. Recently, Weber et al. investigated the helium permeation properties of a palladium membrane fabricated on alumina support by chemical vapor deposition [150]. Similar to H_2, helium permeance across the membrane also showed a clear increment (from 84 to 171 GPU) as the testing temperatures increase from 35 to 188 °C. As the enhancement in He permeance is more significant than N_2, increasing temperature resulted in a slight increase of He/N_2 selectivity. Overall, considering the cost and helium separation performance, the palladium/alumina nano-composite membrane is located at the low end and considered little attractive.

On the other hand, compared to polymeric membranes, the biggest advantage of these inorganic membranes and CMS (section 2.4) is their ability to operate at extreme temperatures and therefore they can be better used within a conventional upgrading process, replacing PSA; polymeric membranes require ambient temperature use –

which represents a significant energy penalty compared to inorganics.

To sum up, some of the above-mentioned inorganic membranes show promising helium separation performances, but more research should be carried out to investigate separation mechanisms, long-term stability at high-temperature conditions, hydrothermal stability, and influence of impurities. Moreover, the upscaling and the cost reduction of inorganic membranes must be further evaluated before bringing them into large-scale applications for helium recovery.

2.6 Mixed matrix membranes

MMMs are hybrid membranes consisting of an organic polymer matrix and an inorganic phase [170]. Some representative examples of fillers commonly employed in MMMs for helium separation have been listed in **Table 5**. The inherent superior separation characteristics of the inorganic phase ensure MMMs' potential to achieve higher selectivity and/or permeability, relative to the existing polymeric membranes. In the meantime, the polymeric matrix maintains good processability and flexibility [171].

Table 5. Category and representative examples of the fillers used in MMMs for helium separation

| Fillers	Representative example
Silica-based	Nanosized Silica
Zeolite	Zeolite L
MOFs	ZIF-8, UiO-66, Cu-BDC

Attempts have been made in applying MMMs in helium separation. The helium separation data of representative MMMs are summarized in **Figure 12**.
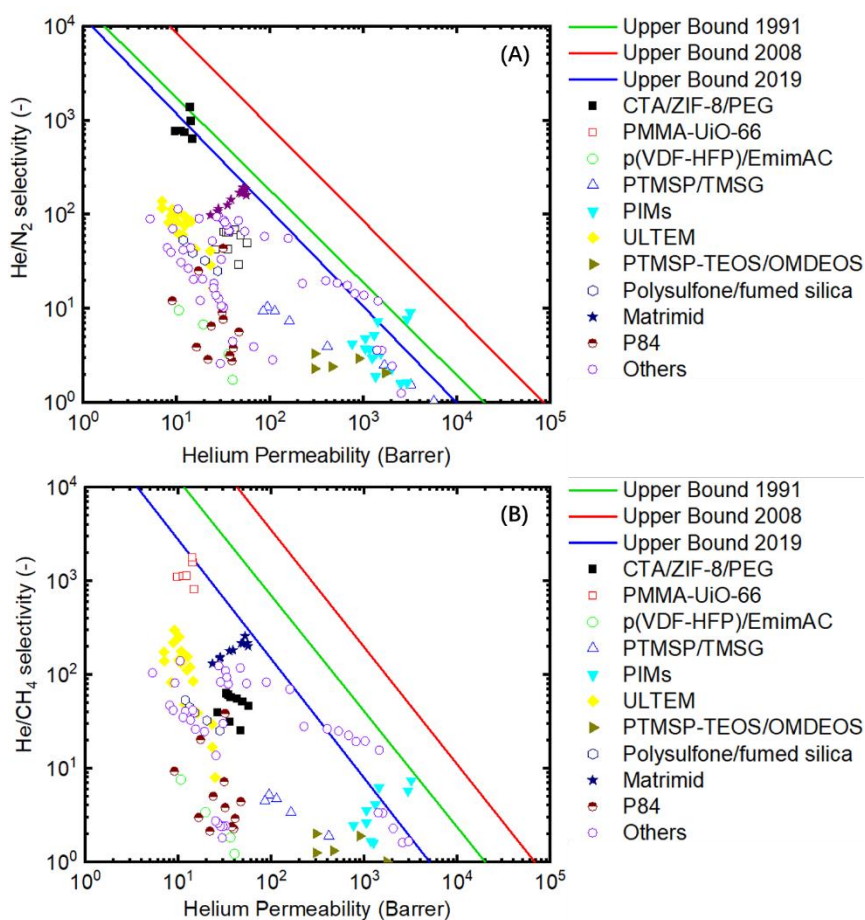
Figure 12. He/N_2 and He/CH_4 separation performances of MMMs.

MOFs are one of the most popular nano additives employed in MMMs fabrication [172]. Various MOFs have been applied in MMMs for helium separation, including ZIF-8 [173, 174], Cu-BTC, Cu-BDC [175], UiO-66 [176, 177], etc. Both Cu-BTC and Cu-BDC have been employed as nano additives in Matrimid® 5218 to improve helium separation performances [175]. Results show that with the addition of both MOFs into Matrimid® 5218 (up to 35 wt.%) increases monotonously the helium permeability, but He/CH_4 and He/N_2 selectivities firstly increase and then slightly fall at 35 wt.%. Besides, Cu-BDC functionalized membranes exhibited greater improvement in both helium permeability and selectivity over N_2 and CH_4 compared with membranes containing Cu-BTC, which is attributed to the better compatibility between Cu-BDC and Matrimid® 5218. In mixed gas permeation tests carried out at 35 °C, 5 bar with He/CH_4 or He/N_2 mixture of 10 % helium as the feed gas, the optimized MMMs (30 wt.% Cu-BDC) displayed 2.4-fold increase in He permeability with around doubled He/N_2 and

He/CH$_4$ selectivity, than neat Matrimid membrane.
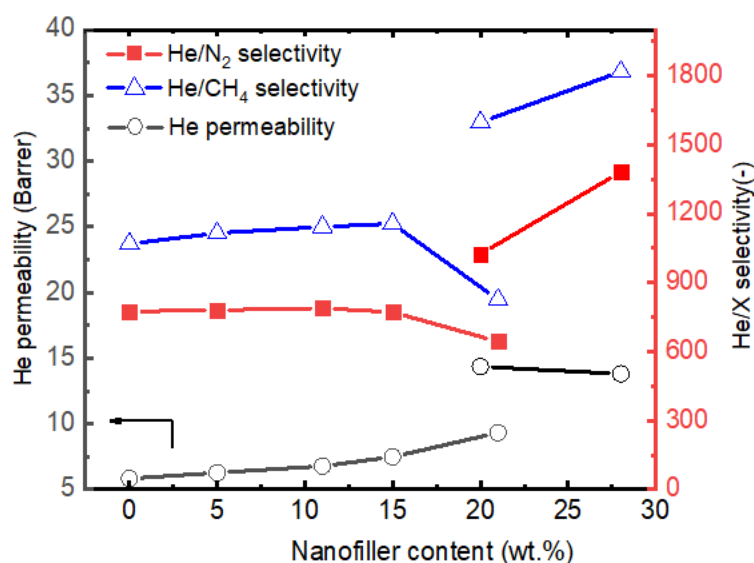
Figure 13. Helium separation performances of MMMs containing functionalized MOFs, replotted
based on data from ref [176] with permission. Copyright (2018) from Wiley.

However, an unexpectedly low selectivity has commonly been reported in many studies,
which is mainly the result of bad compatibility between inorganic fillers and the
polymer matrix. To overcome this issue, nanofillers which are chemically modified or
grafted with an organic layer on their surface have been proposed for better phase
compatibility. Molavi et al. fabricated a series of poly(methyl methacrylate) (PMMA)
based MMMs containing functionalized UiO-66 particles [176]. For unmodified UiO-
66, increasing UiO-66 content from 5 wt.% to 21 wt.% resulted in helium permeability
increasing from 8 Barrer to about 16 Barrer, while greatly decreased He/N$_2$ (~ 630) and
He/CH$_4$ (~ 830) selectivity was observed at 21 wt.% UiO-66 addition. On the other
hand, the MMMs with functionalized UiO-66s presented much higher He/N$_2$ and
He/CH$_4$ selectivity at the same filler content with comparable helium permeability. For
instance, for MMMs with NH$_2$–UiO-66 (20 wt.%), a helium permeability of ~14 Barrer
with He/N$_2$ and He/CH$_4$ selectivity of ~1000 and ~1600 were obtained, respectively (as
shown in **Figure 13**). In the same work, vinyl-functionalized UiO-66 was connected
with PMMA chains through participating in the PMMA polymerization. Its helium
permeability of ~13.8 Barrer with He/N$_2$ and He/CH$_4$ selectivity of ~1400 and ~1800

were achieved, respectively, with the addition of 28 wt.% UiO-66 [176]. Based on the data obtained from this study, it seems to functionalize MOF particles for better filler-matrix compatibility can be an effective approach in enhancing MMMs helium separation performances.

Another approach uses the third compound to fill the nanovoid between fillers and polymeric phase [173]. Polyethylene glycol (PEG) and ZIF-8 were added into cellulose triacetate (CTA) matrix, and experimental results show that the composition of CTA/PEG/ZIF-8 with a weight ratio of 60:20:20 exhibited the most improved performance (P_{He} = 73.25 Barrer) for He/N$_2$ (α = 43) and He/CH$_4$ (α = 40) separations. It is worth mentioning that the authors employed up to 12 different mathematical models to predict the gas separation performance of the obtained MMMs. The classic Maxwell model fitted best and presented the lowest error in predicting the experimental results.

Researchers also tried to make hybrid membranes by adding ionic liquids (ILs) into the Pebax matrix to improve gas separation performances [177]. However, the presence of ILs is more effective in improving the solubility of gases with higher critical temperatures (e.g., CH$_4$ and N$_2$), thus adding ILs into the Pebax matrix resulted in a moderate improvement in helium permeance but a significant increase in both N$_2$ and CH$_4$ permeances, leading to a sharp reduction in the helium selectivities.

Overall, based on the data collected from the available literature, compared to other separation membranes (e.g., carbon membranes and inorganic membranes), it can be concluded that the attempts of preparing hybrid membranes for helium separation are not that successful. Most of the obtained separation results locate below the upper bound proposed by Robeson in 2008 [48], let alone the upper bound proposed in 2019 [49]. Most MMMs generally show high gas permeance but relatively low selectivity. Due to the natural properties of both He/N$_2$ and He/CH$_4$ gas pairs, that is, differences in their kinetic size are much greater than their solubility in polymer-based membranes, the improvement in molecular sizing of the hybrid materials should be more efficient in enhancing the overall selectivity rather than solubility selectivity. However, the

almost unavoidable inter-voids between the nanofiller and polymer matrix result in a non-selective region. Another reason is the reported MMMs normally employ relatively low-performance polymers (e.g., Matrimid, polysulfone (PSf)) as the polymeric matrix. Thus, even though the presence of nanofillers can improve the separation performance, the overall performance is still far away upper bound.

3. Membrane processes for helium recovery

3.1. Membrane process design

Compared to the efforts devoted to new membrane materials, to develop energy-efficient and cost-effective membrane processes for helium recovery from natural gas, process design and optimization are also crucial [37].

He et al. reported that the separation performances of membrane systems are largely dependent on process configurations (**Figure 14A**) [178], and a single-stage membrane unit cannot simultaneously achieve high helium recovery and high purity [179]. Therefore, multi-stage membrane systems are indispensable required to produce high purity helium from natural gas, as shown in **Figure 14B and 14C**. The obtained crude helium in the 1st-stage from the process Option A contains 50~70 % helium, small quantities of CH_4, Ne, and H_2, and balanced N_2, which will be concentrated to be more than 90% helium in the 2nd-stage of the He-upgrading unit. However, for the process Option B, as CH_4 content is high in the 2nd-stage retentate, recycling should be applied to recover CH_4 to avoid significant CH_4 loss, as indicated in **Figure 14C**. It should be noted that using membrane system alone is quite challenging to achieve the helium purity of over 99%. Therefore, cryogenic distillation followed by the catalytic oxidation of H_2 and PSA process is usually employed to remove the impurities (i.e., N_2, CH_4, H_2, and Ne) to produce purified helium of >99.99 %.
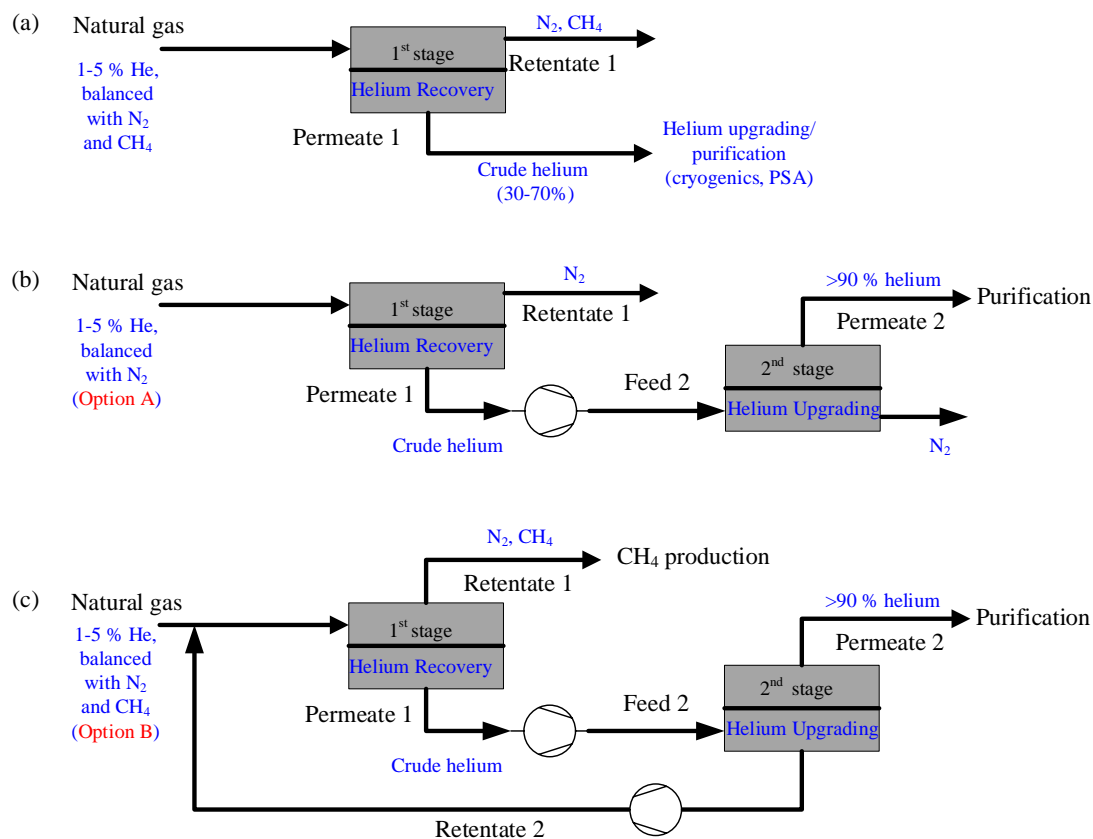
Figure 14. The process design of membrane systems for He recovery

3.2 Technology advances

Process simulation of membrane technology for helium recovery from natural gas or other industrial gas sources has been widely studied and reported in the literature [28, 37, 179-183]. Hägg et al. compared three different types of membranes (i.e., porous silica, CMS, and Matrimid) for their applicability in helium recovery processes [179]. They reported that all three membranes achieve high purity (97 mol.%) and helium recovery (90 %) in a two-stage separation process. Compared to Matrimid membrane, even though silica and CMS membranes are more expensive, the higher helium permeability coupled with higher He/CH_4 and He/N_2 selectivity still makes them more competitive. Moreover, Hamedi et al. also reported a potential capital cost reduction of around 16–30 % using silica membrane system compared to polymeric membrane system, even though silica membrane's price is 60 times higher than polymeric membranes [181]. However, the challenges on the up-scaling of inorganic membranes needs to be addressed for the commercial application in helium recovery. Scholes et al.

claimed that membrane gas separation is economically competitive for direct helium recovery when the natural gas field has a helium concentration of ≥ 0.3 % [180]. Moreover, to make a stand-alone membrane system for helium recovery competitive, the membrane process should achieve a helium purity of >99 mol.% and a recovery of 99 % [50], which is quite challenging for most current polymeric membranes, as their He/N_2 selectivities are below 100 (see **Figure 6**). Scholes et al. also pointed out a clear benefit of increasing helium selectivity over CH_4 or N_2 for the membranes process Option B, as it would expand the membrane market in low-quality natural gas fields [50]. While for the process Option A, after the nitrogen rejection unit (NRU), improving He/N_2 selectivity can only slightly reduce the transmembrane pressure difference (major energy consumption source) [50]. Abdul Quader et al. reported that membrane separation technologies for helium recovery have the potential to be economically viable, as the breakeven price for upgraded helium ($149.89 and $187.81 for one thousand standard cubic feet of 90 % He and 99 % He, respectively) was lower than current market prices [183]. However, future work on developing advanced configurations and membrane materials to reduce compressor power demand is needed to bring down the breakeven price further. **Figure 15** shows the literature summary of the qualitative comparison of membrane technology with other separation methods on energy consumption, cost, footprint, helium purity, helium recovery, environmental impact, and process flexibility characteristics [18]. The choice of suitable separation technology mainly depends on the specific location of the gas plant. Membranes show lower energy consumption, higher process flexibility, and a smaller footprint than other separation methods. However, for a membrane system, the main challenge for helium recovery from natural gas is to obtain high helium purity and recovery simultaneously. Developing novel membrane materials and designing hybrid separation systems may potentially address this issue.
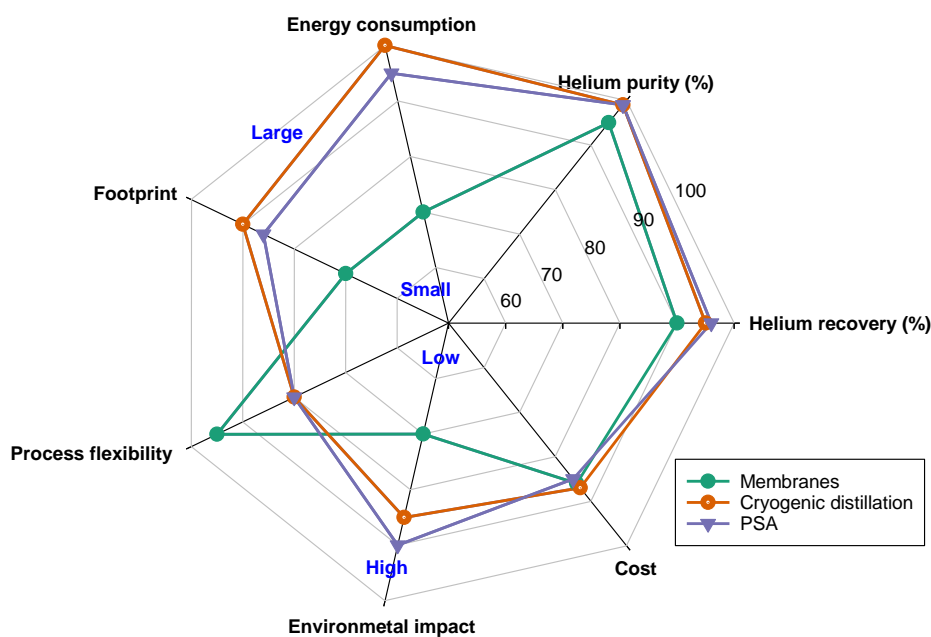
Figure 15. Comparison of membranes with other technologies for helium recovery from natural gas

(adapted from [18]).

4. Challenges and potential solutions of membranes for helium separation

As discussed above, membrane technology presents a promising approach for helium recovery from natural gas. However, it is still challenging to achieve high helium purity even though some newly developed membranes have good He/N_2 and He/CH_4 selectivities (e.g., silica or carbon membranes listed in **Table 3** and **Figure 11**). Moreover, material cost at large-scale production needs to be reduced. Hybrid processes by combining two or more stand-alone separation technologies have attracted great interest due to the potential high energy efficiency compared to a single technology [180, 181, 184]. Scholes et al. reported that for the purification of helium from the nitrogen rejection unit off-gas [180], a hybrid membrane–PSA process is more economical compared with conventional technologies. This study suggests that membrane separation is more economical for bulk helium purification from 1-3 % up to 50-70 %, but to further purify helium to the high purity of >99.99 % will increase the cost dramatically. The challenges and potential solutions related to membrane

materials and module/process developments for helium recovery are summarized in

Table 6. It can be seen that improving material performance should be continuously

pursued to bring down the required membrane area (reflecting the membrane unit cost)

and the operating cost (relevant to the energy consumption for realizing the required

driving force for gas separation). Helium permeance can be notably enhanced by

making CMS membranes into a composite or asymmetric structure. In this case, carbon

hollow fiber membranes may have great potential to address the challenge, thanks to

CMS's high selectivity of helium over N_2 and CH_4 and the easiness of module making

into a hollow fiber configuration with high packing density, and hybrid processes, such

as membrane-cryogenics or membrane-PSA systems, can take advantage of both

membrane separation and PSA or cryogenic distillation.

Table 6. Challenges and potential solutions of membrane systems for helium recovery from natural gas

Challenges	Potential solutions	Remarks
Low He/N_2 and He/CH_4 selectivity	Develop CMS membranes with high selectivity or cheap inorganic membranes	The molecular sieving mechanism provides a high selectivity of helium over larger gas molecules.
Low helium permeance	(1) Fabricate asymmetric or composite membranes	Reduce the thickness of the selective layer.
	(2) Increase the operating temperature	Elevate operation temperature could greatly enhance helium diffusivity with negligible loss of helium solubility
High membrane cost at large scale	(1) Use high packing density hollow fiber configuration;	Silica membranes may be only applicable for small-scale plants due to the difficulty of poor reproducibility.
	(2) Developing cheap but high performances polymers	
A trade-off between helium purity and recovery	(1) Design hybrid systems, such as membrane-cryogenics or membrane-PSA processes.	Combining the advantages of different separation technologies to achieve an energy-efficient separation process
	(2) Process optimization and heat integration	

5. Conclusions and perspectives

The worldwide helium consumption is increasing every year, but the helium production

capacity can barely catch up. Therefore, developing new technologies with low cost

and high efficiency for helium recovery from natural gas is of great importance. In

recent years, recovering helium using membranes has been considered a promising

approach. This review summarized more than 1800 separation data on various membrane materials, including polymeric membranes, carbon membranes, inorganic membranes and mixed matrix membranes. Great progress has been made in the past few decades. However, there is still a big margin for further improvement. In addition, research must be done to tackle the challenges associated with some of the above-mentioned membranes. Based on the current progress, a few perspectives are given on the future development of membrane materials and processes.

First of all, developing new polymeric membrane materials with high separation performance is always desired to reduce helium separation costs. For those developed membranes with sufficient helium permeability and selectivity, exploiting new methods to fabricate them into TFC membranes with enhanced permeance is another critical step. Secondly, some of the CMS membranes already display high permeance and high selectivity; developing CMS membranes using low-cost materials and simple carbonization protocol can be critical points for CMS membrane development. Also, the lifetime of CMS membranes, especially in presence of impurities (e.g., water vapor, high absorbed gases), is another important topic that needs to be investigated.

Thirdly, for silica membranes and zeolite membranes, many promising helium separation data have been reported. Recent progress has also shown a positive trend towards fabrication simplification and microstructure engineering to synthesize thin and oriented membranes. However, emphasis on the reproducibility and stability of performance under multi-component mixtures should remain the focus of fundamental studies. Moreover, the challenge of up-scaling of silica and zeolite membranes needs to be overcome. Membrane formation by processes amenable to continuous processing (e.g., extrusion, spinning, and coating-based) should be the technological focus. In terms of emerging inorganic membrane materials for helium separation, studies should be carried out to investigate the transport mechanism and characterize their membrane microstructures (e.g., preferred orientation, designed interfaces, grain boundary control).

Finally, designing proper hybrid processes such as membrane-cryogenics or membrane-

PSA for helium separation is another direction that should be studied. In the hybrid process, membranes can be used for crude helium separation (from below 1% to 50~70 %), while PSA or cryogenic distillation is responsive for helium purification (from 50~70 % to over 99.9 %). A suitable hybrid process not only improves the separation efficiency but also makes more natural gas reservoirs with low helium concentration economically feasible for helium production.

Abbreviations

Abbreviations	Full name
BN	Boron nitride
CAPEX	Capital cost
CHA	Chabazite
CMS	Carbon molecular sieve
CN	Carbon nitride
CNT	Carbon nanotube
COF	Covalent organic framework
CTA	Cellulose triacetate
Cu-BDC	Copper 1,4-benzenedicarboxylate
Cu-BTC	Copper benzene-1,3,5-tricarboxylate
DDR	Deca-dodecasil 3R
DFT	Density functional theory
FAU	Faujasite
FER	Ferrierite
GO	Graphene oxide
GPU	Gas permeation unit
IL	Ionic liquids
LTA	Linde Type A
MD	Molecular dynamics
MMMs	Mixed matrix membranes
MOFs	Metal organic frameworks
MOR	Mordenite
NMRI	Nuclear Magnetic Resonance Imaging
NCC	Nanocellulose crystals
PAN	Polyacrylonitrile
PBDI	Poly(p-phenylene benzobisimidazole)
PDMS	Polydimethylsiloxane

PEG	Polyethylene glycol
PEI	Polyetherimide
PG	Porous graphene
PI	Polyimide
PIMs	Polymers of intrinsic micro-porosity
PMMA	Poly(methyl methacrylate)
Poly(PFMD)	Poly(perfluoro-2-methylene-1,3-dioxolane)
Poly(PFMMD)	Poly(perfluoro-2-methylene-4-methyl-1,3-dioxolane)
Polysulfone	PSf
PPO	Polyphenylene Oxide
PSA	Pressure Swing Adsorption
PVP	Polyvinyl pyrrolidone
STP	Standard Temperature and Pressure
TFC	Thin-film-composite
ZIF	Zeolitic imidazolate framework

Acknowledgment

References

[1] W.M. "Bo" Sears, What Is Helium?, in: Helium: The Disappearing Element, Springer International Publishing, Cham, 2015, pp. 1-15.

[2] M. Mahesh, P.B. Barker, The MRI helium crisis: past and future, Journal of the American College of Radiology, 13 (2016) 1536-1537.

[3] W.M. Sears, Helium: the disappearing element, Springer International Publishing, New York, NY, USA, 2015.

[4] C.J. Berganza, J.H. Zhang, The role of helium gas in medicine, Medical gas research, 3 (2013) 18.

[5] P.A. Chludzinski, Helium recycling for optical fiber manufacturing, in: U.S.P.a.T. Office (Ed.), Corning Incorporated, United States, 2001.

[6] A. Pinera, Rocket engine propulsion system, in: U.S.P.a.T. Office (Ed.), Florida Turbine Technologies Inc., United State, 2013.

[7] J. Stephens, W. Cartagena, Liquid hydrogen propellant tank sub-surface pressurization with gaseous helium, in: Space, Phoenix, AZ, 2015.

[8] A. Baddeley, J. De Figueredo, J. Hawkswell Curtis, A. Williams, Nitrogen narcosis and performance under water, Ergonomics, 11 (1968) 157-164.

[9] J. Thomas, Reversal of nitrogen narcosis in rats by helium pressure, Undersea biomedical research, 3 (1976) 249.

[10] P. Harris, R. Barnes, The uses of helium and xenon in current clinical practice, Anaesthesia, 63 (2008) 284-293.

[11] W.J. Nuttall, R. Clarke, B. Glowacki, The future of helium as a natural resource, 1st ed., Routledge, London, United Kingdom, 2012.

[12] W.M. Haunschild, Helium purification system for lighter-than-air aircraft, in: U.S.P.a.T. Office (Ed.), United States, 1992.

[13] F.P. Schäfer, Cruise airship with an anchoring device and a helium tempering device, in: U.S.P.a.T. Office (Ed.), Schäfer Fritz Peter, United States, 2001.

[14] G. Baret, R. Gevaud, Helium leak detector, in: U.S.P.a.T. Office (Ed.), Alcatel CIT SA, United States, 1994.

[15] W.G. Bley, Helium leak detectors: from a laboratory device to dedicated industrial leak test units, Vacuum, 44 (1993) 627-632.

[16] W.J. Nuttall, R.H. Clarke, B.A. Glowacki, Stop squandering helium, Nature, 485 (2012) 573-575.

[17] Statista, Distribution of helium consumption worldwide as of 2016, by end use, in, 2017.

[18] T.E. Rufford, K.I. Chan, S.H. Huang, E.F. May, A review of conventional and emerging process technologies for the recovery of helium from natural gas, Adsorption Science & Technology, 32 (2014) 49-72.

[19] Mineral commodity summaries 2021, in: Mineral Commodity Summaries, Reston, VA, 2021, pp. 200.

[20] I. Market, Helium, IHS Markit, 2019.

[21] U.S.D.o.t. Interior, U.S.G. Survey, Mineral Commodity Summaries 2019, in: D.B.J.F.R. II (Ed.) Mineral Commodity Summaries, Reston, VA, 2019, pp. 204.

[22] W.P. Halperin, The impact of helium shortages on basic research, Nature Physics, 10 (2014) 467-470.

[23] D.A. Shea, D.L. Morgan, The helium-3 shortage: Supply, demand, and options for congress, in, Congressional Research Service, Washington, DC, USA, 2010.

[24] A. Cho, Helium-3 Shortage Could Put Freeze On Low-Temperature Research, Science, 326 (2009) 778.

[25] C. Witchalls, Nobel prizewinner: We are running out of helium, New Scientist, 207 (2010) 29.

[26] D. Butler, Qatar blockade hits helium supply, Nature News, 547 (2017) 16.

[27] M. Peplow, US bill would keep helium store afloat, Nature, 497 (2013) 168-169.

[28] M. Alders, D. Winterhalder, M. Wessling, Helium recovery using membrane processes, Separation and Purification Technology, 189 (2017) 433-440.

[29] B.C. Fiedler, J.J. Maloney, J.R. Handley, Cryogenic helium production system, in: U.S.P.a.T. Office (Ed.), Praxair Technology Inc, United States, 1994.

[30] S. Stern, T. Sinclair, P. Gareis, N. Vahldieck, P. Mohr, Helium recovery by permeation, Industrial & Engineering Chemistry, 57 (1965) 49-60.

[31] R.W. Baker, B.T. Low, Gas Separation Membrane Materials: A Perspective, Macromolecules, 47 (2014) 6999-7013.

[32] R.V. Welch, Helium-What About It?, PETSOC-85-05-08, 24 (1985) 3.

[33] V. Martin-Gil, M.Z. Ahmad, R. Castro-Muñoz, V. Fila, Economic Framework of Membrane Technologies for Natural Gas Applications, Separation & Purification Reviews, 48 (2019) 298-324.

[34] C.A. Scholes, G.W. Stevens, S.E. Kentish, Membrane gas separation applications in natural gas processing, Fuel, 96 (2012) 15-28.

[35] J. Sunarso, S.S. Hashim, Y.S. Lin, S.M. Liu, Membranes for helium recovery: An overview on the context, materials and future directions, Separation and Purification Technology, 176 (2017) 335-383.

[36] A. Soleimany, S.S. Hosseini, F. Gallucci, Recent progress in developments of membrane materials and modification techniques for high performance helium separation and recovery: A review, Chemical Engineering and Processing: Process Intensification, 122 (2017) 296-318.

[37] C.A. Scholes, U.K. Ghosh, Review of Membranes for Helium Separation and Purification, Membranes, 7 (2017) 9.

[38] R. Barrer, D. Ibbitson, Occlusion of hydrocarbons by chabazite and analcite, Transactions of the Faraday Society, 40 (1944) 195-206.

[39] P.C. Carman, P.L.R. Malherbe, E.K. Rideal, Diffusion and flow of gases and vapours through micropores II. Surface flow, Proceedings of the Royal Society of London. Series A. Mathematical and Physical Sciences, 203 (1950) 165-178.

[40] P.F. Zito, A. Caravella, A. Brunetti, E. Drioli, G. Barbieri, Knudsen and surface diffusion competing for gas permeation inside silicalite membranes, Journal of Membrane Science, 523 (2017) 456-469.

[41] W.J.W. Bakker, L.J.P. Van Den Broeke, F. Kapteijn, J.A. Moulijn, Temperature dependence of one-component permeation through a silicalite-1 membrane, AIChE Journal, 43 (1997) 2203-2214.

[42] R.W. Baker, Membrane technology and applications, John Wiley & Sons, Chichester, England, 2004.

[43] Membrane Transport Theory, in: Membrane Technology and Applications, 2004, pp. 15-87.

[44] R.M. Barrer, J.A. Barrie, J. Slater, Sorption and diffusion in ethyl cellulose. Part III. Comparison between ethyl cellulose and rubber, Journal of Polymer Science, 27 (1958) 177-197.

[45] P.J. Flory, Principles of polymer chemistry, Cornell University Press, Ithaca, NY, USA, 1953.

[46] A. Fick, Ueber diffusion, Annalen der Physik, 170 (1855) 59-86.

[47] L.M. Robeson, Correlation of separation factor versus permeability for polymeric membranes, Journal of Membrane Science, 62 (1991) 165-185.

[48] L.M. Robeson, The upper bound revisited, Journal of Membrane Science, 320 (2008) 390-400.

[49] A.X. Wu, J.A. Drayton, Z.P. Smith, The perfluoropolymer upper bound, AIChE Journal, 65 (2019) e16700.

[50] C.A. Scholes, U. Ghosh, Helium separation through polymeric membranes: selectivity targets, Journal of Membrane Science, 520 (2016) 221-230.

[51] B. Comesaña-Gándara, J. Chen, C.G. Bezzu, M. Carta, I. Rose, M.-C. Ferrari, E. Esposito, A. Fuoco, J.C. Jansen, N.B. McKeown, Redefining the Robeson upper bounds for CO2/CH4 and CO2/N2 separations using a series of ultrapermeable benzotriptycene-based polymers of intrinsic microporosity, Energy & Environmental Science, 12 (2019) 2733-2740.

[52] N. Belov, Y. Nizhegorodova, A. Zharov, I. Konovalova, V. Shantarovich, Y. Yampolskii, A new polymer, poly (perfluoropropylvinyl ether) and its comparison with other perfluorinated membrane materials, Journal of Membrane Science, 495 (2015) 431-438.

[53] T.C. Merkel, H. Zhang, Z. He, Y. Okamoto, Gas separation membranes based on fluorinated and perfluorinated polymers, in: U.S.P.a.T. Office (Ed.), Membrane Technology and Research Inc. New York University, United States, 2017.

[54] Y. Yampolskii, N. Belov, A. Alentiev, Perfluorinated polymers as materials of membranes for gas and vapor separation, Journal of Membrane Science, 598 (2020) 117779.

[55] T.C. Merkel, I. Pinnau, R. Prabhakar, B.D. Freeman, Gas and vapor transport properties of perfluoropolymers, Materials science of membranes for gas and vapor separation, 1 (2006).

[56] M. Yavari, M. Fang, H. Nguyen, T.C. Merkel, H. Lin, Y. Okamoto, Dioxolane-based perfluoropolymers with superior membrane gas separation properties, Macromolecules, 51 (2018) 2489-2497.

[57] S.M. Nemser, I.C. Roman, Perfluorodioxole membranes, in: W.I.P. Organization (Ed.), Du Pont Canda Inc,

E.I. Du Pont De Nemours And Company, 1991.

[58] M. Macchione, J.C. Jansen, G. De Luca, E. Tocci, M. Longeri, E. Drioli, Experimental analysis and simulation of the gas transport in dense Hyflon® AD60X membranes: influence of residual solvent, Polymer, 48 (2007) 2619-2635.

[59] N. Belov, A. Zharov, A. Shashkin, M. Shaikh, K. Raetzke, Y.P. Yampolskii, Gas transport and free volume in hexafluoropropylene polymers, Journal of membrane science, 383 (2011) 70-77.

[60] R. Nikiforov, N. Belov, A. Zharov, I. Konovalova, B. Shklyaruk, Y. Yampolskii, Gas permeation and diffusion in copolymers of tetrafluoroethylene and hexafluoropropylene: effect of annealing, Journal of Membrane Science, 540 (2017) 129-135.

[61] J.S. Chiou, D.R. Paul, Gas permeation in a dry Nafion membrane, Industrial & engineering chemistry research, 27 (1988) 2161-2164.

[62] J. Catalano, T. Myezwa, M. De Angelis, M.G. Baschetti, G. Sarti, The effect of relative humidity on the gas permeability and swelling in PFSI membranes, International journal of hydrogen energy, 37 (2012) 6308-6316.

[63] N. Belov, R. Nikiforov, E. Polunin, Y. Pogodina, I. Zavarzin, V. Shantarovich, Y. Yampolskii, Gas permeation, diffusion, sorption and free volume of poly (2-trifluoromethyl-2-pentafluoroethyl-1, 3-perfluorodioxole), Journal of Membrane Science, 565 (2018) 112-118.

[64] X. Wang, M. Shan, X. Liu, M. Wang, C.M. Doherty, D. Osadchii, F. Kapteijn, High-Performance Polybenzimidazole Membranes for Helium Extraction from Natural Gas, ACS Applied Materials & Interfaces, 11 (2019) 20098-20103.

[65] S.-H. Choi, M.M.B. Sultan, A.A. Alsuwailem, S.M. Zuabi, Preparation and characterization of multilayer thin-film composite hollow fiber membranes for helium extraction from its mixtures, Separation and Purification Technology, 222 (2019) 152-161.

[66] G. Dibrov, M. Ivanov, M. Semyashkin, V. Sudin, G. Kagramanov, High-Pressure Aging of Asymmetric Torlon® Hollow Fibers for Helium Separation from Natural Gas, Fibers, 6 (2018) 83.

[67] D.A. Syrtsova, M.G. Shalygin, V.V. Teplyakov, Fluorinated Hollow Fiber Membranes Based on Matrimid 5218 and Their Application in the Process of Helium Recovery from Natural Gas, Petroleum Chemistry, 58 (2018) 760-769.

[68] P.K. Gantzel, U. Merten, Gas Separations with High-Flux Cellulose Acetate Membranes, Industrial & Engineering Chemistry Process Design and Development, 9 (1970) 331-332.

[69] M.L. Jue, V. Breedveld, R.P. Lively, Defect-free PIM-1 hollow fiber membranes, Journal of Membrane Science, 530 (2017) 33-41.

[70] C.W. Jones, W.J. Koros, Carbon molecular sieve gas separation membranes-I. Preparation and characterization based on polyimide precursors, Carbon, 32 (1994) 1419-1425.

[71] G. Bernardo, T. Araújo, T. da Silva Lopes, J. Sousa, A. Mendes, Recent advances in membrane technologies for hydrogen purification, International Journal of Hydrogen Energy, 45 (2020) 7313-7338.

[72] N. Sazali, M.A. Mohamed, W.N.W. Salleh, Membranes for hydrogen separation: a significant review, The International Journal of Advanced Manufacturing Technology, 107 (2020) 1859-1881.

[73] S.P. Cardoso, I.S. Azenha, Z. Lin, I. Portugal, A.E. Rodrigues, C.M. Silva, Inorganic Membranes for Hydrogen Separation, Separation & Purification Reviews, 47 (2018) 229-266.

[74] R. Ash, R. Barrer, R. Lowson, Diffusion of helium through a microporous carbon membrane, Surface science, 21 (1970) 265-272.

[75] L. Lei, L. Bai, A. Lindbråthen, F. Pan, X. Zhang, X. He, Carbon membranes for CO_2 removal: Status and perspectives from materials to processes, Chemical Engineering Journal, 401 (2020) DOI:10.1016/j.cej.2020.126084.

[76] K. Hazazi, X. Ma, Y. Wang, W. Ogieglo, A. Alhazmi, Y. Han, I. Pinnau, Ultra-selective carbon molecular sieve membranes for natural gas separations based on a carbon-rich intrinsically microporous polyimide precursor, Journal of Membrane Science, 585 (2019) 1-9.

[77] L. Lei, F. Pan, A. Lindbråthen, X. Zhang, M. Hillestad, Y. Nie, L. Bai, X. He, M.D. Guiver, Carbon hollow fiber membranes for a molecular sieve with precise-cutoff ultramicropores for superior hydrogen separation, Nature Communications, 12 (2021) 268.

[78] Y.K. Kim, H.B. Park, Y.M. Lee, Gas separation properties of carbon molecular sieve membranes derived from polyimide/polyvinylpyrrolidone blends: effect of the molecular weight of polyvinylpyrrolidone, Journal of Membrane Science, 251 (2005) 159-167.

[79] A.B. Fuertes, D.M. Nevskaia, T.A. Centeno, Carbon composite membranes from Matrimid® and Kapton® polyimides for gas separation, Microporous and Mesoporous Materials, 33 (1999) 115-125.

[80] W. Ogieglo, A. Furchner, X. Ma, K. Hazazi, A.T. Alhazmi, I. Pinnau, Thin Composite Carbon Molecular Sieve Membranes from a Polymer of Intrinsic Microporosity Precursor, ACS Applied Materials & Interfaces, 11 (2019) 18770-18781.

[81] A.B. Fuertes, T.A. Centeno, Preparation of supported carbon molecular sieve membranes, Carbon, 37 (1999) 679-684.

[82] S.C. Rodrigues, M. Andrade, J. Moffat, F.D. Magalhães, A. Mendes, Preparation of carbon molecular sieve membranes from an optimized ionic liquid-regenerated cellulose precursor, Journal of Membrane Science, 572 (2019) 390-400.

[83] L. Lei, A. Lindbråthen, X. Zhang, E.P. Favvas, M. Sandru, M. Hillestad, X. He, Preparation of carbon molecular sieve membranes with remarkable CO_2/CH_4 selectivity for high-pressure natural gas sweetening, Journal of Membrane Science, 614 (2020) DOI:0.1016/j.memsci.2020.118529.

[84] M.B. Rao, S. Sircar, Nanoporous carbon membranes for separation of gas mixtures by selective surface flow, Journal of Membrane Science, 85 (1993) 253-264.

[85] H.B. Park, Y.M. Lee, Fabrication and Characterization of Nanoporous Carbon/Silica Membranes, Advanced Materials, 17 (2005) 477-483.

[86] E.P. Favvas, N.S. Heliopoulos, S.K. Papageorgiou, A.C. Mitropoulos, G.C. Kapantaidakis, N.K. Kanellopoulos, Helium and hydrogen selective carbon hollow fiber membranes: The effect of pyrolysis isothermal time, Separation and Purification Technology, 142 (2015) 176-181.

[87] E.P. Favvas, E.P. Kouvelos, G.E. Romanos, G.I. Pilatos, A.C. Mitropoulos, N.K. Kanellopoulos, Characterization of highly selective microporous carbon hollow fiber membranes prepared from a commercial co-polyimide precursor, Journal of Porous Materials, 15 (2008) 625-633.

[88] J.N. Barsema, N.F.A. van der Vegt, G.H. Koops, M. Wessling, Carbon molecular sieve membranes prepared from porous fiber precursor, Journal of Membrane Science, 205 (2002) 239-246.

[89] M.A. Mohamed, N. Sazali, Polyimide-based Carbon Membrane: Effect of Coating Times on Helium Separations, Journal of Advanced Research in Applied Mechanics, 64 (2019) 1-6.

[90] N. Sazali, W.N.W. Salleh, A.F. Ismail, K. Kadirgama, F.E.C. Othman, P84 Co-Polyimide Based-Tubular Carbon Membrane: Effect of Heating Rates on Helium Separations, Solid State Phenomena, 280 (2018) 308-311.

[91] N. Sazali, W.N.W. Salleh, A.F. Ismail, Carbon tubular membranes from nanocrystalline cellulose blended with P84 co-polyimide for H_2 and He separation, International Journal of Hydrogen Energy, 42 (2017) 9952-9957.

[92] N. Sazali, W.N.W. Salleh, A.F. Ismail, N.H. Ismail, N. Yusof, F. Aziz, J. Jaafar, K. Kadirgama, Influence of intermediate layers in tubular carbon membrane for gas separation performance, International Journal of Hydrogen Energy, 44 (2019) 20914-20923.

[93] J. Su, A.C. Lua, Effects of carbonisation atmosphere on the structural characteristics and transport properties of carbon membranes prepared from Kapton® polyimide, Journal of Membrane Science, 305 (2007) 263-270.

[94] S. Khan, K. Wang, X. Feng, A. Elkamel, Carbon molecular sieve membranes for natural gas purification: Role of surface flow, The Canadian Journal of Chemical Engineering, 98 (2020) 775-784.

[95] I. Kumakiri, K. Tamura, Y. Sasaki, K. Tanaka, H. Kita, Influence of Iron Additive on the Hydrogen Separation Properties of Carbon Molecular Sieve Membranes, Industrial & Engineering Chemistry Research, 57 (2018) 5370-5377.

[96] S.C. Rodrigues, R. Whitley, A. Mendes, Preparation and characterization of carbon molecular sieve membranes based on resorcinol–formaldehyde resin, Journal of Membrane Science, 459 (2014) 207-216.

[97] P.-S. Lee, D. Kim, S.-E. Nam, R.R. Bhave, Carbon molecular sieve membranes on porous composite tubular supports for high performance gas separations, Microporous and Mesoporous Materials, 224 (2016) 332-338.

[98] W. Zhou, M. Yoshino, H. Kita, K.-i. Okamoto, Preparation and gas permeation properties of carbon molecular sieve membranes based on sulfonated phenolic resin, Journal of Membrane Science, 217 (2003) 55-67.

[99] S.J. Fishlock, S.H. Pu, G. Bhattacharya, Y. Han, J. McLaughlin, J.W. McBride, H.M.H. Chong, S.J. O'Shea, Micromachined nanocrystalline graphite membranes for gas separation, Carbon, 138 (2018) 125-133.

[100] W. Ogieglo, T. Puspasari, X. Ma, I. Pinnau, Sub-100 nm carbon molecular sieve membranes from a polymer of intrinsic microporosity precursor: Physical aging and near-equilibrium gas separation properties, Journal of Membrane Science, 597 (2020) 117752.

[101] W. Ogieglo, T. Puspasari, M.K. Hota, N. Wehbe, H.N. Alshareef, I. Pinnau, Nanohybrid thin-film composite carbon molecular sieve membranes, Materials Today Nano, 9 (2020) 100065.

[102] H.-J. Lee, M. Yoshimune, H. Suda, K. Haraya, Gas permeation properties of poly(2,6-dimethyl-1,4-phenylene oxide) (PPO) derived carbon membranes prepared on a tubular ceramic support, Journal of Membrane Science, 279 (2006) 372-379.

[103] T.A. Centeno, A.B. Fuertes, Carbon molecular sieve gas separation membranes based on poly(vinylidene chloride-co-vinyl chloride), Carbon, 38 (2000) 1067-1073.

[104] W. Mi, Y.S. Lin, Y. Li, Vertically aligned carbon nanotube membranes on macroporous alumina supports, Journal of Membrane Science, 304 (2007) 1-7.

[105] J.B.S. Hamm, A.R. Muniz, L.D. Pollo, N.R. Marcilio, I.C. Tessaro, Experimental and computational analysis of carbon molecular sieve membrane formation upon polyetherimide pyrolysis, Carbon, 119 (2017) 21-29.

[106] D. Parsley, R.J. Ciora, D.L. Flowers, J. Laukaitaus, A. Chen, P.K.T. Liu, J. Yu, M. Sahimi, A. Bonsu, T.T. Tsotsis, Field evaluation of carbon molecular sieve membranes for the separation and purification of hydrogen from coal- and biomass-derived syngas, Journal of Membrane Science, 450 (2014) 81-92.

[107] Evonik, P84® Polyimides - A unique high-performance polymer in, 2019.

[108] N. Sazali, W. Salleh, A. Ismail, N. Ismail, F. Aziz, N. Yusof, H. Hasbullah, Effect of stabilization temperature during pyrolysis process of P84 co-polyimide-based tubular carbon membrane for H2/N2 and He/N2 separations, in: IOP Conference Series: Materials Science and Engineering, IOP Publishing, 2018, pp. 012027.

[109] G. Gavalas, C. Megiris, S. Nam, Deposition of H2-permselective SiO2 films, Chemical engineering science, 44 (1989) 1829-1835.

[110] C.E. Megiris, J.H. Glezer, Synthesis of hydrogen-permselective membranes by modified chemical vapor deposition. Microstructure and permselectivity of silica/carbon/Vycor membranes, Industrial & engineering chemistry research, 31 (1992) 1293-1299.

[111] R. Uhlhorn, K. Keizer, A. Burggraaf, Gas transport and separation with ceramic membranes. Part II. Synthesis and separation properties of microporous membranes, Journal of membrane science, 66 (1992) 271-287.

[112] R. De Lange, J. Hekkink, K. Keizer, A. Burggraaf, Formation and characterization of supported microporous ceramic membranes prepared by sol-gel modification techniques, Journal of membrane science, 99 (1995) 57-75.

[113] R.M. De Vos, H. Verweij, High-selectivity, high-flux silica membranes for gas separation, Science, 279 (1998) 1710-1711.

[114] S. Kitao, M. Asaeda, Separation of organic acid/water mixtures by thin porous silica membrane, Journal of chemical engineering of Japan, 23 (1990) 367-370.

[115] H. Van Veen, Y. Van Delft, C. Engelen, P. Pex, Dewatering of organics by pervaporation with silica membranes, Separation and Purification Technology, 22 (2001) 361-366.

[116] M.C. Duke, J.D. Da Costa, D.D. Do, P.G. Gray, G.Q. Lu, Hydrothermally robust molecular sieve silica for wet gas separation, Advanced Functional Materials, 16 (2006) 1215-1220.

[117] A.I. Labropoulos, G.E. Romanos, N. Kakizis, G.I. Pilatos, E.P. Favvas, N.K. Kanellopoulos, Investigating the evolution of N2 transport mechanism during the cyclic CVD post-treatment of silica membranes, Microporous and Mesoporous Materials, 110 (2008) 11-24.

[118] J. Lei, H. Song, Y. Wei, S. Zhao, H. Qi, A novel strategy to enhance hydrothermal stability of Pd-doped organosilica membrane for hydrogen separation, Microporous and Mesoporous Materials, 253 (2017) 55-63.

[119] M. Kanezashi, K. Yada, T. Yoshioka, T. Tsuru, Design of Silica Networks for Development of Highly Permeable Hydrogen Separation Membranes with Hydrothermal Stability, Journal of the American Chemical Society, 131 (2009) 414-415.

[120] Y. Gu, P. Hacarlioglu, S.T. Oyama, Hydrothermally stable silica–alumina composite membranes for hydrogen separation, Journal of Membrane Science, 310 (2008) 28-37.

[121] J. Caro, M. Noack, P. Kölsch, R. Schäfer, Zeolite membranes – state of their development and perspective, Microporous and Mesoporous Materials, 38 (2000) 3-24.

[122] I. Wenten, P. Dharmawijaya, P. Aryanti, R. Mukti, LTA zeolite membranes: current progress and challenges in pervaporation, RSC advances, 7 (2017) 29520-29539.

[123] I. Kumakiri, Y. Sasaki, W. Shimidzu, K. Hashimoto, H. Kita, T. Yamaguchi, S.-i. Nakao, Micro-structure change of polycrystalline FAU zeolite membranes during a hydrothermal synthesis in a dilute solution, Microporous and Mesoporous Materials, 272 (2018) 53-60.

[124] A. Tavolaro, A. Julbe, C. Guizard, A. Basile, L. Cot, E. Drioli, Synthesis and characterization of a mordenite membrane on an α-Al2O3 tubular support, Journal of Materials Chemistry, 10 (2000) 1131-1137.

[125] A. Brunetti, M. Migliori, D. COZZA, E. Catizzone, G. Giordano, G. Barbieri, Methanol conversion to Dimethyl ether in Catalytic zeolite membrane reactors, ACS Sustainable Chemistry & Engineering, (2020).

[126] J. Caro, J. Kärger, From computer design to gas separation, Nature Materials, 19 (2020) 374-375.

[127] P. Kumar, D.W. Kim, N. Rangnekar, H. Xu, E.O. Fetisov, S. Ghosh, H. Zhang, Q. Xiao, M. Shete, J.I. Siepmann, One-dimensional intergrowths in two-dimensional zeolite nanosheets and their effect on ultra-selective transport, Nature materials, 19 (2020) 443-449.

[128] S. Imasaka, M. Itakura, K. Yano, S. Fujita, M. Okada, Y. Hasegawa, C. Abe, S. Araki, H. Yamamoto, Rapid preparation of high-silica CHA-type zeolite membranes and their separation properties, Separation and Purification Technology, 199 (2018) 298-303.

[129] K. Kida, Y. Maeta, K. Yogo, Preparation and gas permeation properties on pure silica CHA-

type zeolite membranes, Journal of Membrane Science, 522 (2017) 363-370.

[130] N. Chang, H. Tang, L. Bai, Y. Zhang, G. Zeng, Optimized rapid thermal processing for the template removal of SAPO-34 zeolite membranes, Journal of Membrane Science, 552 (2018) 13-21.

[131] S.F. Alam, M.-Z. Kim, Y.J. Kim, A. ur Rehman, A. Devipriyanka, P. Sharma, J.-G. Yeo, J.-S. Lee, H. Kim, C.-H. Cho, A new seeding method, dry rolling applied to synthesize SAPO-34 zeolite membrane for nitrogen/methane separation, Journal of Membrane Science, 602 (2020) 117825.

[132] Y. Zhang, S. Chen, R. Shi, P. Du, X. Qiu, X. Gu, Pervaporation dehydration of acetic acid through hollow fiber supported DD3R zeolite membrane, Separation and Purification Technology, 204 (2018) 234-242.

[133] Y. Liu, B. Zhang, D. Liu, P. Sheng, Z. Lai, Fabrication and molecular transport studies of highly c-oriented AFI membranes, Journal of Membrane Science, 528 (2017) 46-54.

[134] J. Caro, M. Noack, Zeolite membranes – Recent developments and progress, Microporous and Mesoporous Materials, 115 (2008) 215-233.

[135] N. Kosinov, J. Gascon, F. Kapteijn, E.J. Hensen, Recent developments in zeolite membranes for gas separation, Journal of Membrane Science, 499 (2016) 65-79.

[136] M. Simplício, M.D. Afonso, O. Borisevich, X. Lefebvre, D. Demange, Permeation of single gases and binary mixtures of hydrogen and helium through a MFI zeolite hollow fibres membrane for application in nuclear fusion, Separation and Purification Technology, 122 (2014) 199-205.

[137] S.A.S. Rezai, J. Lindmark, C. Andersson, F. Jareman, K. Möller, J. Hedlund, Water/hydrogen/hexane multicomponent selectivity of thin MFI membranes with different Si/Al ratios, Microporous and mesoporous materials, 108 (2008) 136-142.

[138] R. Antunes, A. Böhmländer, A. Bükki-Deme, B. Krasch, M.M. Cruz, L. Frances, Experimental investigation of the ideal selectivity of MFI-ZSM-5 zeolite-type membranes for a first evaluation of the separation of hydrogen isotopologues from helium, Separation and Purification Technology, 212 (2019) 767-773.

[139] S. Denning, J. Lucero, C.A. Koh, M.A. Carreon, Chabazite Zeolite SAPO-34 Membranes for He/CH4 Separation, ACS Materials Letters, 1 (2019) 655-659.

[140] B. Liu, R. Zhou, K. Yogo, H. Kita, Preparation of CHA zeolite (chabazite) crystals and membranes without organic structural directing agents for CO2 separation, Journal of Membrane Science, 573 (2019) 333-343.

[141] T. Tomita, K. Nakayama, H. Sakai, Gas separation characteristics of DDR type zeolite membrane, Microporous and Mesoporous Materials, 68 (2004) 71-75.

[142] X. Wang, Y. Zhang, X. Wang, E. Andres-Garcia, P. Du, L. Giordano, L. Wang, Z. Hong, X. Gu, S. Murad, Xenon recovery by DD3R zeolite membranes: application in anaesthetics, Angewandte Chemie, 131 (2019) 15664-15671.

[143] C. Chen, A. Ozcan, A.O. Yazaydin, B.P. Ladewig, Gas permeation through single-crystal ZIF-8 membranes, Journal of Membrane Science, 575 (2019) 209-216.

[144] O. Kadioglu, S. Keskin, Efficient separation of helium from methane using MOF membranes, Separation and Purification Technology, 191 (2018) 192-199.

[145] F. Cao, C. Zhang, Y. Xiao, H. Huang, W. Zhang, D. Liu, C. Zhong, Q. Yang, Z. Yang, X. Lu, Helium Recovery by a Cu-BTC Metal–Organic-Framework Membrane, Industrial & Engineering Chemistry Research, 51 (2012) 11274-11278.

[146] C. Athanasekou, M. Pedrosa, T. Tsoufis, L.M. Pastrana-Martínez, G. Romanos, E. Favvas, F.

Katsaros, A. Mitropoulos, V. Psycharis, A.M.T. Silva, Comparison of self‐standing and supported graphene oxide membranes prepared by simple filtration: Gas and vapor separation, pore structure and stability, Journal of Membrane Science, 522 (2017) 303-315.

[147] G. Li, K. Zhang, T. Tsuru, Two‐Dimensional Covalent Organic Framework (COF) Membranes Fabricated via the Assembly of Exfoliated COF Nanosheets, ACS Applied Materials & Interfaces, 9 (2017) 8433-8436.

[148] Y. Wang, J. Li, Q. Yang, C. Zhong, Two‐Dimensional Covalent Triazine Framework Membrane for Helium Separation and Hydrogen Purification, ACS Applied Materials & Interfaces, 8 (2016) 8694-8701.

[149] J.S. Roh, H. Lee, T.H. Lee, H.W. Yoon, T.H. Choi, S.‐H. Do, S.Y. Yoo, B.D. Freeman, T. Song, U. Paik, H.B. Park, Unprecedentedly Low CO2 Transport through Vertically Aligned, Conical Silicon Nanotube Membranes, Nano Letters, 20 (2020) 4754-4760.

[150] M. Weber, M. Drobek, B. Rebière, C. Charmette, J. Cartier, A. Julbe, M. Bechelany, Hydrogen selective palladium‐alumina composite membranes prepared by Atomic Layer Deposition, Journal of Membrane Science, 596 (2020) 117701.

[151] Q.‐L. Zhu, Q. Xu, Metal–organic framework composites, Chemical Society Reviews, 43 (2014) 5468-5512.

[152] C. Altintas, S. Keskin, Molecular simulations of MOF membranes and performance predictions of MOF/polymer mixed matrix membranes for CO2/CH4 separations, ACS sustainable chemistry & engineering, 7 (2018) 2739-2750.

[153] Z. Rui, J.B. James, A. Kasik, Y. Lin, Metal‐organic framework membrane process for high purity CO2 production, AIChE Journal, 62 (2016) 3836-3841.

[154] J. Hou, Y. Wei, S. Zhou, Y. Wang, H. Wang, Highly efficient H2/CO2 separation via an ultrathin metal-organic framework membrane, Chemical Engineering Science, 182 (2018) 180-188.

[155] K. Yang, Y. Ban, A. Guo, M. Zhao, Y. Zhou, N. Cao, W. Yang, In‐situ interfacial assembly of ultra-H2-permeable metal-organic framework membranes for H2/CO2 separation, Journal of Membrane Science, (2020) 118419.

[156] W. Wu, Z. Li, Y. Chen, W. Li, Polydopamine‐Modified Metal–Organic Framework Membrane with Enhanced Selectivity for Carbon Capture, Environmental science & technology, 53 (2019) 3764-3772.

[157] V. Chernikova, O. Shekhah, Y. Belmabkhout, M. Eddaoudi, Nanoporous Fluorinated Metal‐Organic Framework-Based Membranes for CO2 Capture, ACS Applied Nano Materials, (2020).

[158] X. Jiang, S. Li, Y. Bai, L. Shao, Ultra‐facile aqueous synthesis of nanoporous zeolitic imidazolate framework membranes for hydrogen purification and olefin/paraffin separation, Journal of Materials Chemistry A, 7 (2019) 10898-10904.

[159] R. Wei, H.Y. Chi, X. Li, D. Lu, Y. Wan, C.W. Yang, Z. Lai, Aqueously Cathodic Deposition of ZIF-8 Membranes for Superior Propylene/Propane Separation, Advanced Functional Materials, 30 (2020) 1907089.

[160] Y. Yoo, V. Varela-Guerrero, H.-K. Jeong, Isoreticular metal− organic frameworks and their membranes with enhanced crack resistance and moisture stability by surfactant‐assisted drying, Langmuir, 27 (2011) 2652-2657.

[161] R. Ranjan, M. Tsapatsis, Microporous metal organic framework membrane on porous support using the seeded growth method, Chemistry of Materials, 21 (2009) 4920-4924.

[162] S. Takamizawa, Y. Takasaki, R. Miyake, Single-crystal membrane for anisotropic and efficient gas permeation, Journal of the American Chemical Society, 132 (2010) 2862-2863.

[163] B.M. Yoo, J.E. Shin, H.D. Lee, H.B. Park, Graphene and graphene oxide membranes for gas separation applications, Current opinion in chemical engineering, 16 (2017) 39-47.

[164] H. Huang, Y. Ying, X. Peng, Graphene oxide nanosheet: an emerging star material for novel separation membranes, Journal of Materials Chemistry A, 2 (2014) 13772-13782.

[165] Q. Xu, H. Xu, J. Chen, Y. Lv, C. Dong, T.S. Sreeprasad, Graphene and graphene oxide: advanced membranes for gas separation and water purification, Inorganic Chemistry Frontiers, 2 (2015) 417-424.

[166] R. Joshi, S. Alwarappan, M. Yoshimura, V. Sahajwalla, Y. Nishina, Graphene oxide: the new membrane material, Applied Materials Today, 1 (2015) 1-12.

[167] T. Van Gestel, J. Barthel, New types of graphene-based membranes with molecular sieve properties for He, H2 and H2O, Journal of Membrane Science, 554 (2018) 378-384.

[168] J. Zhu, X. Meng, J. Zhao, Y. Jin, N. Yang, S. Zhang, J. Sunarso, S. Liu, Facile hydrogen/nitrogen separation through graphene oxide membranes supported on YSZ ceramic hollow fibers, Journal of Membrane Science, 535 (2017) 143-150.

[169] F.A. Nezhad, N. Han, Z. Shen, Y. Jin, Y. Wang, N. Yang, S. Liu, Experimental and theoretical exploration of gas permeation mechanism through 2D graphene (not graphene oxides) membranes, Journal of Membrane Science, 601 (2020) 117883.

[170] M. Galizia, W.S. Chi, Z.P. Smith, T.C. Merkel, R.W. Baker, B.D. Freeman, 50th anniversary perspective: polymers and mixed matrix membranes for gas and vapor separation: a review and prospective opportunities, Macromolecules, 50 (2017) 7809-7843.

[171] M. Vinoba, M. Bhagiyalakshmi, Y. Alqaheem, A.A. Alomair, A. Pérez, M.S. Rana, Recent progress of fillers in mixed matrix membranes for CO2 separation: A review, Separation and Purification Technology, 188 (2017) 431-450.

[172] Y. Wang, X. Wang, J. Guan, L. Yang, Y. Ren, N. Nasir, H. Wu, Z. Chen, Z. Jiang, 110th Anniversary: Mixed matrix membranes with fillers of intrinsic nanopores for gas separation, Industrial & Engineering Chemistry Research, 58 (2019) 7706-7724.

[173] A. Soleimany, J. Karimi-Sabet, S.S. Hosseini, Experimental and modeling investigations towards tailoring cellulose triacetate membranes for high performance helium separation, Chemical Engineering Research and Design, 137 (2018) 194-212.

[174] A.F. Bushell, M.P. Attfield, C.R. Mason, P.M. Budd, Y. Yampolskii, L. Starannikova, A. Rebrov, F. Bazzarelli, P. Bernardo, J. Carolus Jansen, M. Lanč, K. Friess, V. Shantarovich, V. Gustov, V. Isaeva, Gas permeation parameters of mixed matrix membranes based on the polymer of intrinsic microporosity PIM-1 and the zeolitic imidazolate framework ZIF-8, Journal of Membrane Science, 427 (2013) 48-62.

[175] A. Akbari, J. Karimi-Sabet, S.M. Ghoreishi, Matrimid® 5218 based mixed matrix membranes containing metal organic frameworks (MOFs) for helium separation, Chemical Engineering and Processing - Process Intensification, 148 (2020) 107804.

[176] H. Molavi, A. Shojaei, S.A. Mousavi, Improving mixed-matrix membrane performance via PMMA grafting from functionalized NH2–UiO-66, Journal of Materials Chemistry A, 6 (2018) 2775-2791.

[177] J.C. Jansen, K. Friess, G. Clarizia, J. Schauer, P. Izák, High Ionic Liquid Content Polymeric Gel Membranes: Preparation and Performance, Macromolecules, 44 (2011) 39-45.

[178] X. He, M.-B. Hägg, T.-J. Kim, Hybrid FSC membrane for CO_2 removal from natural gas: Experimental, process simulation, and economic feasibility analysis, AIChE Journal, 60 (2014) 4174-4184.

[179] M.-B. Hagg, A. Lindbrathen, S. Haider, M. Saeed, Techno-economic evaluation of helium recovery from natural gas; A comparison between inorganic and polymeric membrane technology, Journal of Membrane Science and Research, 5 (2019) 126-136.

[180] C.A. Scholes, U.K. Gosh, M.T. Ho, The Economics of Helium Separation and Purification by Gas Separation Membranes, Industrial & Engineering Chemistry Research, 56 (2017) 5014-5020.

[181] H. Hamedi, I.A. Karimi, T. Gundersen, A novel cost-effective silica membrane-based process for helium extraction from natural gas, Computers & Chemical Engineering, 121 (2019) 633-638.

[182] C.A. Scholes, Helium Recovery through Inorganic Membranes Incorporated with a Nitrogen Rejection Unit, Industrial & Engineering Chemistry Research, 57 (2018) 3792-3799.

[183] M.A. Quader, T.E. Rufford, S. Smart, Modeling and cost analysis of helium recovery using combined-membrane process configurations, Separation and Purification Technology, 236 (2020) 116269.

[184] M.M. Shah, J.M. Schwartz, K. Koita, M.J. Dray, Integrated process and apparatus for recovery of helium rich streams, in: U.S.P.a.T. Office (Ed.), Praxair Technology Inc., United States, 2017.